Plant Physiology and Biochemistry 231 (2026) 110958

Contents lists available at ScienceDirect

Plant Physiology and Biochemistry

journal homepage: www.elsevier.com/locate/plaphy

Natural variability in *Olea europaea* L. reveals diverse functional strategies to drought under a CO_2-enriched atmosphere

I. Aranda [a,*], D. Sánchez-Gómez [a], F.J. Cano [a], L. Quintanilla [b], M. Del Rey-Granado [a], P. Díaz-Rueda [c], J.M. Colmenero-Flores [c], B. Fernandez de Simón [a], N. Fernandez del Saz [e], M. Ribas-Carbó [e], J. Gago [d,e]

[a] Instituto de Ciencias Forestales (ICIFOR-INIA), CSIC. Ctra. La Coruña km 7.5, 28040 Madrid. Spain
[b] Global Change Research Institute, University Rey Juan Carlos, 28933, Móstoles, Spain
[c] Instituto de Recursos Naturales y Agrobiología, Consejo Superior de Investigaciones Científicas (CSIC), Seville, 41012, Spain
[d] Agro-Environmental and Water Economics Institute (INAGEA), University of the Balearic Islands, 07122, Palma de Mallorca, Spain
[e] Departament de Biologia, Universitat de les Illes Balears, Carretera de Valldemossa Km 7.5, 07122, Palma de Mallorca, Illes Balears, Spain

ARTICLE INFO

Keywords:
Olea europaea
Water stress
CO_2
Gas exchange
Water consumption
Water use efficiency
Ci
Drought
$\delta^{13}C$
$\delta^{15}N$

ABSTRACT

The wild olive (*Olea europaea* L.) is one of the most iconic Mediterranean forest tree species and the ancestor of many cultivated olive varieties. In this study, twelve wild olive genotypes from three distinct subspecies (subsp. *europaea*, subsp. *guanchica*, and subsp. *maroccana*) were grown under ambient ($[CO_2]_{amb}$) and enriched CO_2 atmospheres ($[CO_2]_{enr}$), subject to two watering regimes (WW – Well-watered/WS – Water-stressed). We measured water use at leaf and whole-plant levels, along with growth traits, leaf gas exchange, and leaf isotopic carbon ($\delta^{13}C$) and nitrogen composition ($\delta^{15}N$), to differentiate functional strategies among genotypes in response to CO_2 and soil water availability. Growth under $[CO_2]_{enr}$ lessened water stress effects by increasing water use efficiency (WUE). The improved WUE came from reduced water consumption at both leaf and plant levels under $[CO_2]_{enr}$, although sensitivities to soil water content varied among genotypes. Growth-related traits responded more to water stress than to CO_2. Patterns of N^{15} isotopic composition ($\delta^{15}N$) and total leaf nitrogen content on a mass and area basis (N_{mass} and N_{area}) varied among genotypes in response to atmospheric CO_2 and water stress. A negative relationship between $\delta^{13}C$ and $\delta^{15}N$ indicates a complex interaction between carbon and nitrogen metabolisms under the influence of water availability and CO_2 supply. Our study shows that (1) the response of wild olive to atmospheric CO_2 enrichment is strongly influenced by resource availability, especially water, and (2) it is necessary to consider genotype- and subspecies-specific responses when predicting vegetation response in a CO_2-enriched world.

1. Introduction

Most Mediterranean plant species have evolved adaptations to cope with the seasonal water shortage typical of this ecosystem. However, the increasing intensity and frequency of dry periods are becoming one of the most serious environmental threats to Mediterranean flora (Jacobsen and Pratt, 2018; Forner et al., 2018; Hartmann et al., 2022; Aranda et al., 2024; Mas et al., 2024). Moreover, the intensification of drought impacts occurs concurrently with the progressive enrichment of CO_2 in the atmosphere and other processes affecting the nitrogen cycle (Peñuelas et al., 2020). Conversely, enhanced CO_2 levels in the atmosphere might buffer, to some extent, the adverse effects on plants of rising temperatures and declining precipitation. Nonetheless, the exact outcomes of this interaction remain uncertain (Ainsworth and Long, 2021).

Rising CO_2 levels might induce higher net primary productivity under non-stressful conditions (Beerling et al., 1996; Wullschleger et al., 2002; Wang et al., 2022; Cui et al., 2024; Norby et al., 2024). The increase in total leaf area can contribute to higher C uptake despite a down-regulation of photosynthetic capacity (Wang et al., 2022). In turn, the increase in carbon partitioning to leaf biomass can ultimately lead to higher plant water losses through transpiration. The trade-off between increased leaf biomass and partial stomatal closure due to CO_2 enrichment of the environment is central to the discussion on the potential role

* Corresponding author.
E-mail address: aranda@inia.csic.es (I. Aranda).

https://doi.org/10.1016/j.plaphy.2025.110958
Received 24 October 2025; Received in revised form 7 December 2025; Accepted 15 December 2025
Available online 19 December 2025

of CO_2 in regulating plant water balance (Becklin et al., 2017). However, this issue remains unclear to date, and the debate continues over the universal physiological responses of plants to rising atmospheric CO_2 (Duan et al., 2015; Birami et al., 2020; Lauriks et al., 2022; Norby et al., 2024).

Different specific patterns of physiological response arise from the interaction of atmospheric CO_2 and other climate drivers (Becklin et al., 2017; Duan et al. 2018; Aranda et al., 2020; Jiang et al., 2021; Lauriks et al., 2022), and are species-specific in most cases (Birami et al., 2020). In the case of water availability, this specificity in the response to the co-occurrence of enriched CO_2 atmospheres and reduced water availability reaches intraspecific variation, with different responses according to genotype (Sánchez-Gómez et al., 2017; Lauriks et al., 2022).

During drought, there is a reduction in leaf stomatal conductance, potentially lowering C_i and CO_2 availability at the sites of carboxylation in the chloroplasts (Chaves et al., 2009; Brodribb and McAdam, 2017). Additionally, partial stomatal closure occurs under CO_2-enriched conditions, though it is not universally recognized (Ainsworth and Rogers, 2007; reviewed recently in Ainsworth and Long, 2021; Jiang et al., 2021). However, this may be offset in CO_2-enriched atmospheres due to increased CO_2 around the leaves (i.e. C_a), which can enhance CO_2 assimilation. Yet, the response might, as a result, come across as antagonistic to the observed downregulation of the net carbon uptake capacity of plants under high CO_2 due to nitrogen limitations (Adam et al., 2004; Ellsworth et al., 2004; Ofori-Amanfo et al., 2023). Nonetheless, carbon uptake may still be enhanced by the greater CO_2 availability in leaf intercellular spaces, due to the buildup of carbon source, even after accounting for diffusional limitation by stomata and biochemical down-regulation of carbon assimilation (Kelly et al., 2016). Ultimately, the close coupling of A_{net} and g_{wv} through different atmospheric [CO_2] levels can alter the relatively constant C_i/C_a (Norman, 1982), and often result in increased intrinsic leaf water use efficiency (WUE_i), despite opposing physiological processes. Nevertheless, this apparent homeostatic performance is not universal (Voelker et al., 2016).

Increased WUE is a common response in water-deficient plants, reflected by an enrichment in C^{13} (i.e., increase of $\delta^{13}C$). Regardless of the varying effects of different physiological processes on WUE_i, it is necessary to assess the potential buffering of drought under CO_2 enrichment, considering the whole plant (Jiang et al., 2021). The issue becomes more complex in forest tree species, whose physiological responses are expressed over long time scales. Therefore, $\delta^{13}C$ and WUE_i can be modulated in response to the CO_2 x drought interaction over time in different ways depending on the ontogenic state, acclimation process in the long term and the weight of each environmental factor as main driver of the response. For instance, Birami et al. (2020) recently showed a moderate impact of CO_2 as drought intensified, whereas in other cases the specific response relied on processes of acclimation and was species-specific (Kelly et al., 2016).

Nitrogen is a key nutrient for plant growth (Tegeder and Masclaux-Daubresse, 2018), and its foliar concentration decreases under atmospheric CO_2 enrichment is often reported (Coleman et al., 1993; Crous et al., 2019). Furthermore, carbon uptake capacity can be altered by changes in leaf N stoichiometry and the C: N ratio, which are affected by growing under CO_2 enrichment (Poorter et al., 2022). Changes in N uptake or dilution of N due to biomass accumulation result in lower available N for investment in Rubisco, the main sink of nitrogen in plants (Evans, 1989). The $\delta^{15}N$ of leaves relates to nitrogen uptake. Variations in leaf $\delta^{15}N$ result from complex discrimination processes during nitrogen uptake, arising from biological processes (Craine et al., 2015), abiotic factors such as temperature (Wang, 2024), and different enzymatic isotopic discrimination during nitrogen metabolism in the plant (Tcherkez, 2011). Nevertheless, the importance of $\delta^{15}N$ in response to drought is little studied, and its response to CO_2 enrichment is virtually absent from the literature (Craine et al., 2015). Notably, this lack of information persists even in cases of high connectivity between physiological processes, as illustrated by the interplay between WUE_i and the photosynthetic nitrogen use efficiency (PNUE), or the direct N relationship with the leaf biochemistry involved in carbon uptake and PNUE. It is relevant to point out that changes are observed not only in the water and carbon economies of plants, but also in their nitrogen use. Recent research highlights nitrogen's critical role in the response to atmospheric CO_2 enrichment, as a modulator of plant growth.

Polyploidization, i.e., whole-genome duplication, is another factor that can influence responses to increased CO_2 and reduced water availability. Although numerous studies have shown increased tolerance to abiotic stresses associated with polyploidization in both agronomic (Sattler et al., 2016) and wild plants (e.g., Ramsey, 2011), the consequences of polyploidization on the combined effects of elevated CO_2 and drought remain largely unknown. The *Olea europaea L. complex* (Oleaceae) provides an ideal model to address this issue, as it has diversified through polyploidization and is adapted to prolonged drought events. This complex of small evergreen trees includes both wild and cultivated Mediterranean olives (*O. europaea* subsp. *europaea*), as well as six non-Mediterranean subspecies (Julca et al., 2023). The functional response to drought of different *O. europaea* genotypes from different subspecies has been previously studied under ambient CO_2 conditions (Hernandez-Santana et al., 2019). However, there is a risk of intensified dry spells occurring in the future, coinciding with an increase in the CO_2 levels in the atmosphere. Therefore, the impact of drought and CO_2 has been profusely studied in forest tree species (Scarascia-Mugnozza et al., 1996), and even in the cultivated olive (Tognetti et al., 2001).

The Mediterranean wild olive (*Olea europaea* subsp. *europaea* var. *sylvestris*) forms forests, generally mixed with other Mediterranean tree species, and is the origin of the cultivated olive (var. *europaea*) after a long-term process of domestication (Besnard et al., 2013). This wild olive has a complex evolutionary history with three main long-term lineages from before Quaternary (Besnard et al., 2013, 2018), and frequent introgression processes between wild and cultivated olive varieties (Julca et al., 2023), or between different wild varieties (Díaz-Rueda et al., 2020). The var. *sylvestris* harbors high genetic variation (Belaj et al., 2011), and is the infraspecific taxon with the widest range of distribution (Besnard et al., 2013; 2013). *O. europaea* subsp. *guanchica* is mainly present in the Canary Islands, in the Gomera Island (Díaz-Rueda et al., 2020). The Moroccan olive, *O. europaea* subsp. *maroccana* is only present in the south-eastern part of Morocco (Medeiros and Ward, 2013). Phylogenomic analyses indicate that subspp. *europaea* and *guanchica* are closely related diploid lineages, whereas subsp. *maroccana* represents an allohexaploid taxon whose genome comprises contributions from the *guanchica* lineage and another divergent ancestor (Julca et al., 2023). This work aimed to evaluate the response of different genotypes from these three subspecies to drought under CO_2 enrichment of the atmosphere. We established as working hypotheses: i) the application of moderate water stress to wild olives is mitigated to a certain extent by the growth under CO_2-enriched atmosphere; ii) water economy and nitrogen leaf content are both affected by the interaction between water stress and CO_2 of the atmosphere; iii) Subspecies and genotype-based variability, including differences in ploidy level, result in differential response to drought under elevated CO_2 due to contrasting functional and morphological traits.

2. Material and methods

The experiments were conducted using plants obtained through *in vitro* propagation of 12 *Olea europaea* genotypes selected from the SILVOLIVE collection (Díaz-Rueda et al., 2020). These genotypes were propagated vegetatively, rooted and acclimatised to *ex vitro* conditions following the protocols described by Díaz-Rueda et al. (2020, 2021). Five genotypes belonged to the diploid subsp. *europea* (ACZ), four to the diploid subsp. *guanchica* (HER) and three to the allohexaploid subsp. *maroccana* (MAR). Each genotype was codified with the acronyms of the subspecies followed by a number. Further details on the biogeography

and phylogenetic relationships among the three subspecies are provided in Díaz-Rueda et al. (2020) and in Supplementary Material S1.

Twelve biological replicates of the 12 genotypes were obtained from rooted cuttings and potted into 7.5 L pots. The substrate used for potting was a mix of peat and sand (2:1) with 2.5 g L^{-1} of slow-release fertiliser (Osmocote Plus fertiliser (16-9-12 NPK + micronutrients, Scotts, Heerlen, Netherlands)). The set of plants was divided in two groups, and each one was distributed in two walk-in climatic chambers (Supplementary Photo 1, 26–27 November 2020). Each chamber maintained the same environmental conditions of temperature, vapour pressure deficit, and photoperiod but differed in the [CO_2] of the air surrounding the plants: 400 ppm and 800 ppm. The photoperiod was set at 14 h light/10 h dark. Climate parameters within the walk-in chambers were set to achieve 2 KPa of vapour pressure deficit during daylight (28 °C ±, with 50 % relative humidity), and a PPFD of 700 ± 127 μmol m^{-2} s^{-1} at the plant tips. During the dark phase, conditions were 20.0 ± 0.4 °C and 60.0 ± 1.1 % relative humidity. The 12 clonal replicates per genotype were divided into four groups based on the treatment combination (Watering x CO_2), with three replicates for each combination, 12 plants per genotype across watering and CO_2 treatments. Plants were arranged in three blocks within each chamber (one plant per genotype and watering treatment in each block). Their positions were periodically randomised throughout the experiment. Half of the plants were maintained under well-watered (WW) conditions throughout, while the other half underwent a drought cycle in two steps. After transplanting, all plants were well-watered three times weekly for three months. Subsequently, half of the plants (Water Stress, WS) were subjected to water deficit by withholding watering until soil moisture reached 40 % of the soil moisture holding capacity. These WS plants experienced this stress for a month, after which watering was further withdrawn until the soil moisture dropped to 5–10 %. Plants were kept under this reduced soil moisture for an additional month. We did not directly measure leaf water potential; instead, we relied on soil VWC and leaf water content (WCs) as integrative indicators of plant water status over the duration of the drought treatment. Weighing of the pots and periodic soil moisture measurements with Time Domain Reflectometry (TDR), using TDR probes (CS650-L, Campbell Scientific Inc.) connected to a datalogger (CR1000, Campbell Scientific), allowed for precise control of water stress during both drought phases. Control plants remained well-watered two to three times throughout the experiment to ensure adequate soil moisture. Plants were moved between the walk-in chambers twice during the experiment, maintaining the specific conditions of each CO_2 treatment by reprogramming the chambers to the new CO_2 and maintaining the rest of the environmental conditions, just after reallocation of the plants. This was done the same day, just after the physical change of plants from one of the chambers to the other one. Furthermore, the position of the plants within each block was changed randomly once every two weeks.

2.1. Leaf gas exchange

Leaf gas exchange was measured at different times throughout the experiment at the early, middle and end of the water deficit period (mid-April to the last week of May). The leaf gas exchange and chlorophyll fluorescence were measured 1 h from the start of the light period in one well-differentiated leaf per plant from the third top of the plants with a portable photosynthesis system (LiCor 6400 XP, Li-COR Inc., Lincoln, NE, USA) coupled to an integrated fluorescence chamber (chamber Li-6400-40, Li-COR Inc.). The photosynthetic photon flux density (PPFD) into the exchange chamber during measurements was set to 1200 μmol m^{-2} s^{-1}, temperature to 25 °C and vapour pressure deficit (VPD) ~ 1.2 KPa, as this setting was tested to be effective for saturating photosynthesis and optimum for leaf stomatal conductance. The CO_2 during measurements was the same as that of growing conditions. Gas exchange was recalculated based on the leaf area enclosed within the gas exchange chamber and corrected for potential leakages (Flexas et al., 2007) and for the cuticular conductance to water vapour (g_{min}) following Warren et al. (2011). Cuticular, sometimes called minimal, residual or epidermal, conductance to water vapour was determined according to the free bench dehydration technique, as in Araus et al. (1991), which essentially measures fresh leaf weight lost through the epidermis at regular steps in darkness and under controlled air conditions (wind speed, relative humidity and temperature). Boundary layer conductance was measured by replicating the shape and size of each leaf on saturated wet paper under the same conditions and subtracted to the total leaf transpiration rate, although the effect of the boundary layer on g_{min} was minimal.

2.2. Plant growth and biomass

Six times throughout the experiment, and in monthly intervals, the main height (H) and root collar diameter (D) of plants were measured on all the plants. The D was measured with a digital caliper (±0.01 mm), and H with a ruler (±0.25 cm). The basal area of the plants (BA) was estimated from the diameter measured periodically as $BA = \pi (D/2)^2$. At the end of the experiment, plants were harvested, and above and below-ground tissues were split according to organ. Leaves and main stems were considered separately. The number of secondary shoots born from the main stem was counted on each plant (NS). Total biomass (TB) was estimated as the sum of total root biomass (TRB), stem biomass (TSB) and leaf biomass (TLB) after drying the different fractions in an oven for 48 h at 65 °C. A sub-sample of leaves was scanned to measure leaf area (LA) before determining its dry weight (DW), and used to calculate the specific leaf area (SLA) as the ratio between LA/DW. The SLA of the sub-sample of leaves was calculated and used to estimate the total leaf area (TLA) of the plant by multiplying SLA by TLB. Investment of biomass in different organs was considered from the leaf weight ratio (LWR), stem weight ratio (SWR) and root weight ratio (RWR) estimated from the investment of biomass in the different fractions, relative to total plant biomass. The leaf area ratio (LAR) was estimated from TLA and TB as TLA/TB. We considered most of the stem base as hydraulically functional, and the Huber value (H_v) was calculated from the ratio of the basal area at the base of the stem and the TLA. Table S1 summarizes briefly the different functional traits and their units.

2.3. Isotopic composition and intrinsic water use efficiency

Three-four oven-dry leaves per plant were ground with a ball mill, and ~3.5 mg of each leaf sample were encapsulated in tin capsules. Samples were combusted in an elemental analyser (ThermoFlash EA 1112 Series, Bremen, Germany), and CO_2 and N_2 were directly injected into a continuous-flow isotope ratio mass spectrometer (Thermo-Finnigan Delta XP, Bremen, Germany) to estimate total C and N mass, and $\delta^{13}C$ and $\delta^{15}N$ content of each leaf sample. Peach leaf standards (NIST 1547) were run every six samples. The standard deviation of the analysis was below 0.1 ‰. As is commonly reported, $\delta^{15}N$ was expressed relative to atmospheric N_2 isotopic composition (‰), whereas the $\delta^{13}C$ of samples was reported relative to a synthetic analogue of the Vienna Pee Dee Belemnite standard (VPDB). $\delta^{13}C$ was used as an integrative estimator of WUE_i in the whole leaf.

2.4. Whole-plant water consumption

Volumetric water content of pot soils (VWC) was monitored for each plant regularly throughout the full experiment by soil moisture sensors of 40 cm length (CS650-L, Campbell Scientific Inc., Logan, UT, USA) connected to data loggers (CR1000, Campbell Scientific). Whole-plant level specific water consumption (WC_s) was determined for all the studied plants at three measuring times within the period between 3 March and June 1, 2021 (see below), together with measurements of volumetric water content of pots (VWC). The first WC_s measurement was taken before the application of water deficit, while the last two measurements were taken after the application of the medium and intense

water deficit. Water deficit started on 7th April. WC_s was calculated for each measuring time as:

$$WC_s = \frac{(pW_{t+1} - pW_t)}{(t_{+1} - t)\pi r^2}$$

Where *WCs* is whole-plant level specific water consumption (ml cm^{-2} day^{-1}), pW_t and pW_t indicate pot weight at time t and time t_{+1}, respectively, corresponding to a 1-day interval between pot weights for all measuring times. Losses due to evaporation were negligible over 24 h. Finally, πr^2 denotes the cross-sectional area of the stem at the root collar. Thus, WC_s was standardised by the stem transversal section at the base of the plants, making the WC_s comparable for plants of different sizes and belonging to different genotypes.

Henceforth, all the different morpho-physiological, biochemical and growth-related traits are noted with abbreviations (see the list in Supplementary Table S1).

2.5. Statistical approach

Mixed models were used to evaluate whether gas exchange traits changed across genotypes, watering and CO_2 growing atmosphere (considered as fixed factors). The individual was considered a random factor. We employed a General Linear Model (GLM) framework to assess the effects of experimental factors and covariates on specific water consumption rates. The model incorporated three fixed factors: Watering regime (well watered, WW vs. water stressed, WS levels), growth CO_2 concentration (ambient, 400 ppm vs. elevated 800 ppm), and genotype (12 different genotypic variants), along with their potential interactions. Covariates included Leaf Area Ratio (LAR), stomatal conductance at peak water deficit (g_{wv}), and cuticular conductance (g_{min}).

The assumptions of normality and homoscedasticity were evaluated through graphical diagnostics of the residuals from the best-fitting model. To meet these assumptions, the dependent variable (specific water consumption) was Box-Cox transformed. Model selection was based on Akaike (AIC) and Bayesian (BIC) information criteria. Type III ANOVA was used to evaluate the significance of the different factors and covariates included in the models.

The assumptions of normality and homoscedasticity were evaluated through graphical diagnostics of the residuals from the best-fitting model. To meet these assumptions, the dependent variable (specific water consumption) was Box-Cox transformed. Model selection was based on Akaike (AIC) and Bayesian (BIC) information criteria. Type III ANOVA was used to evaluate the significance of the different factors and covariates included in the models. A gamma probability distribution function was assumed for WCs as it gave the best fit among other distributions (normal, log-normal, Weibull, etc). The shape of the relationship between WCs and VWC for each genotype x CO_2 level combination was analysed by testing different response curves that were parameterized through maximum likelihood using a simulated annealing algorithm. R (R_Core_Team, 2021) was used for the analyses including the R package "likelihood" (Murphy, 2015).

We also performed a principal components analysis (PCA) including the whole of the gas exchange and growth variables as explicative variables. The first three components were used to identify separation among genotypes, watering regime and $[CO_2]$ treatments.

Because of differences in the C^{13} depletion of the atmosphere between the CO_2-enriched and ambient treatments, plant individual values of leaf $\delta^{13}C$ were standardised by the great overall average $\delta^{13}C_{leaf}$ on each CO_2 treatment for statistical purposes [$\delta^{13}C_{standarised}$]. The relationships between $\delta^{13}C_{standarised}$ and WUE_i and C_i/C_a were explored with linear models. Absolute $\delta^{13}C$ values for each treatment are shown in Fig. 4A and Fig. S8, whereas $\delta^{13}C$ standardised is used to compare relative drought responses across CO_2 treatments by removing the $\delta^{13}C$ baseline offset of the air between $[CO_2]_{amb}$ and $[CO_2]_{enr}$.

3. Results

3.1. Leaf gas exchange

Water stress and CO_2 had a notable impact on several traits, as 11 and 12 traits were significantly affected by water stress and CO_2, respectively (Supplementary Table S2). However, the genotype accounted for most of the variation in the set of morpho-physiological and growth-related traits that were examined. A smaller number of significant two- and three-way interactions between the main factors were also observed (Supplementary Table S2).

The A_{net} increased under $[CO_2]_{enr}$ compared to $[CO_2]_{amb}$, and decreased in WS compared to WW plants, significantly in the majority of genotypes (Fig. 1A), but A_{net} of WS plants under $[CO_2]_{enr}$ was higher than WS plants under $[CO_2]_{amb}$. The three genotypes from MAR showed the highest A_{net} across watering and CO_2 treatments. Genotypes from the other subspecies were more variable, except ACZ9, which showed a performance similar to that of genotypes from MAR. A_{net} ranged from 50.84 ± 3.29 μmol m^{-2} s^{-1} in genotype M2 under $[CO_2]_{enr}$ and WW, and 0.69 ± 3.21 μmol m^{-2} s^{-1} in genotype ACZ8 under $[CO_2]_{amb}$ and WS across the different watering x CO_2 treatments. The ETR and R_d followed similar patterns to A_{net} with significant changes among genotypes. However, the response to water stress and CO_2 across genotypes was significant and more variable, with a lower or absent effect of watering and CO_2 (Fig. 1B and C). The three genotypes from MAR and ACZ9 were again the genotypes with the highest ETR and Rd. The g_{wv} was very responsive to watering as it decreased for the majority of genotypes in response to water stress, as much under $[CO_2]_{amb}$ or $[CO_2]_{enr}$. Although water stress was the main abiotic factor impinging g_{wv}, CO_2 affected also the g_{wv} in some genotypes. Thus, higher g_{wv} was recorded in some of the genotypes (ACZ3, HER5 and all MAR genotypes) for WW and $[CO_2]_{amb}$ plants when compared with WW and $[CO_2]_{enr}$ ones (Fig. 1D).

3.2. Relationship of A_{net} with g_{wv} and ETR impact on leaf WUEi and $\delta^{13}C$

There was a positive relationship between A_{net} and g_{wv} across genotypes in the four combinations of CO_2 and watering treatments (Fig. 2A). The highest change of A_{net} with g_{wv} was under $[CO_2]_{enr}$ and WS, and the lowest $[CO_2]_{amb}$ and WW (i.e. higher and lower slopes respectively in the relationship A_{net} *vs* g_{wv}). Thus, the reactivity of A_{net} and the WUE_i (i.e. slope of the $A_{net} - g_{wv}$ relationship in Fig. 2A) to the CO_2 across genotypes was highest when growing under $[CO_2]_{enr}$, and especially when submitted to water stress. The WUEi for all genotypes varied accordingly (Supplementary Fig. S1). The changes in WUEi followed in the majority of the genotypes the same ranking across combination of treatments: $[CO_2]_{enr}$_WS > $[CO_2]_{amb}$_WS ≥ $[CO_2]_{enr}$_WW > $[CO_2]_{amb}$_WW (Supplementary Fig. S1). Improvement in the WUE_i with water stress and $[CO_2]_{enr}$ was not only related to diffusional factors, but also to photochemical ones. Therefore, A_{net} was positively related to ETR across genotypes in the four treatments. The sensitivity of A_{net} to an incremental change in the ETR (i.e. slope of the A_{net}-ETR relationship) across the pool of genotypes was systematically lower under WS, regardless of the $[CO_2]$ level. However, it was higher under $[CO_2]_{enr}$ when comparing within the same watering regime (Fig. 2B).

3.3. Leaf morphology and biochemistry

The genotype was the factor that had a higher impact on SLA, beyond water stress or CO_2 (Supplementary Table S2, Fig. 3A), ranging from 92.7 ± 4.6 cm^2 g^{-1} in HER8 (WW_ $[CO_2]_{amb}$) to 48.8 ± 0.4 cm^2 g^{-1} in ACZ1 (WS _ $[CO_2]_{enr}$) across the different watering x $[CO_2]$ treatments. Watering was the second most important factor in explaining variations across genotypes (Supplementary Table S2). SLA was highest for leaves on most WW plants in both CO_2-growing environments. CO_2 significantly affected the SLA, but only after considering all the genotypes

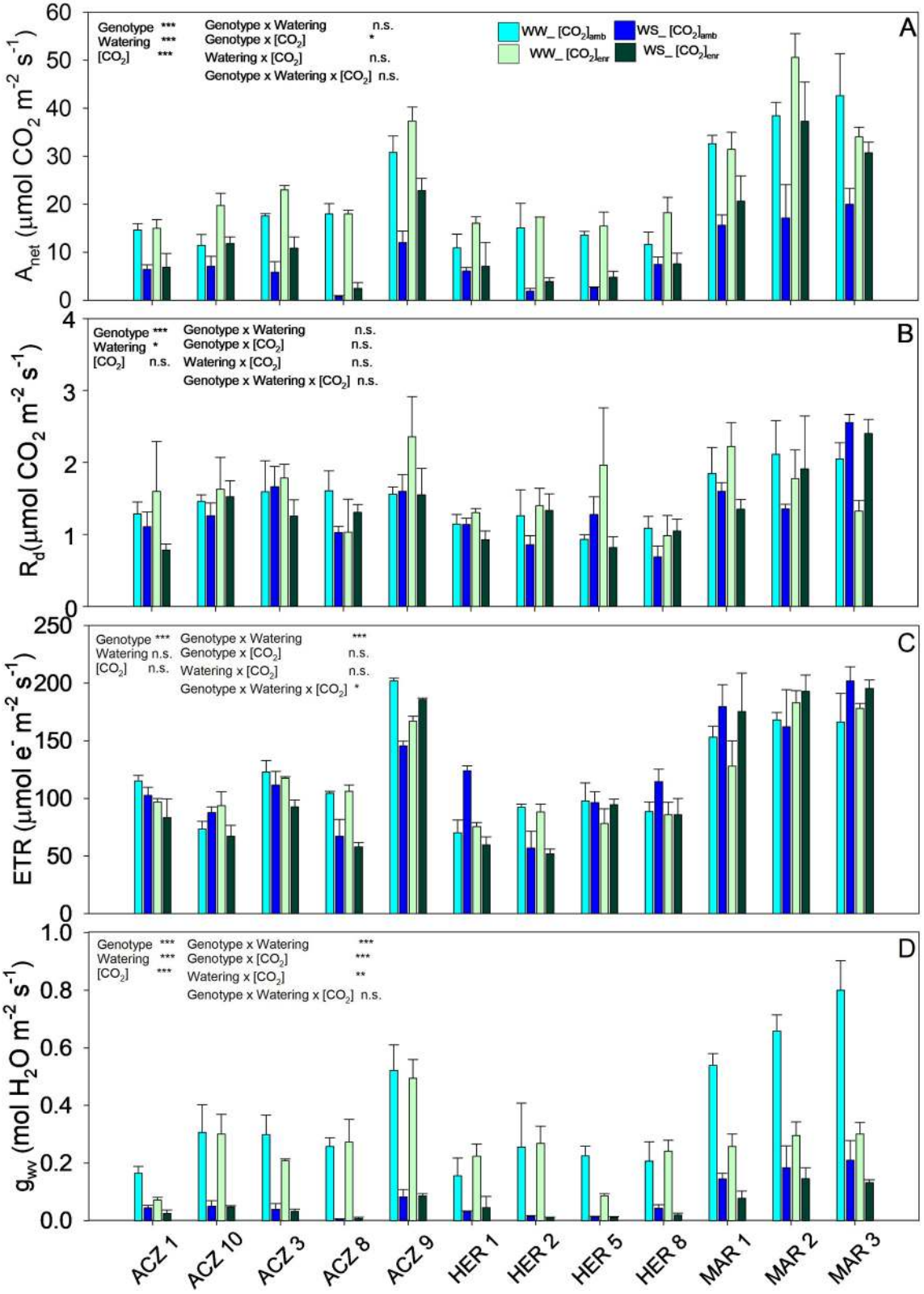

Fig. 1. Variability of leaf gas exchange and chlorophyll fluorescence derived variables according to genotype, water and CO_2 treatments: (A) Net photosynthesis/A_{net}; (B) – dark respiration/R_d; (C) – stomatal conductance to water vapour/g_{wv}; (D) - electron transport rate/ETR. Physiological traits were measured in 12 genotypes from 3 subspecies of *O. europaea* (*europaea, guanchica, maroccana*) submitted to drought (WS) or well-watered (WW), and growing under CO_2 ambient ($[CO_2]_{amb}$/400 ppm) or CO_2 enriched ($[CO_2]_{enr}$/800 ppm) atmospheres. Genotypes: ACZ1, ACZ10, ACZ3, ACZ8, ACZ9 subsp. *europaea*; HER1, HER2, HER5, HER8 subsp. *guanchica*; MAR1, MAR2, MAR3 subsp. *maroccana*. Clear-blue: WW – $[CO_2]_{amb}$; dark-blue: WS-$[CO_2]_{amb}$; Clear-green WW – $[CO_2]_{enr}$; Dark –green, WS – $[CO_2]_{enr}$. Significance of the different factors from lineal models was indicated as: $P < 0.001$ - ***, $P < 0.01$ - **, $P < 0.05$ – *, $P > 0.05$ - n.s., non-significant. Bars indicate average values ± S.E. (n = 3). (For interpretation of the references to colour in this figure legend, the reader is referred to the Web version of this article.)

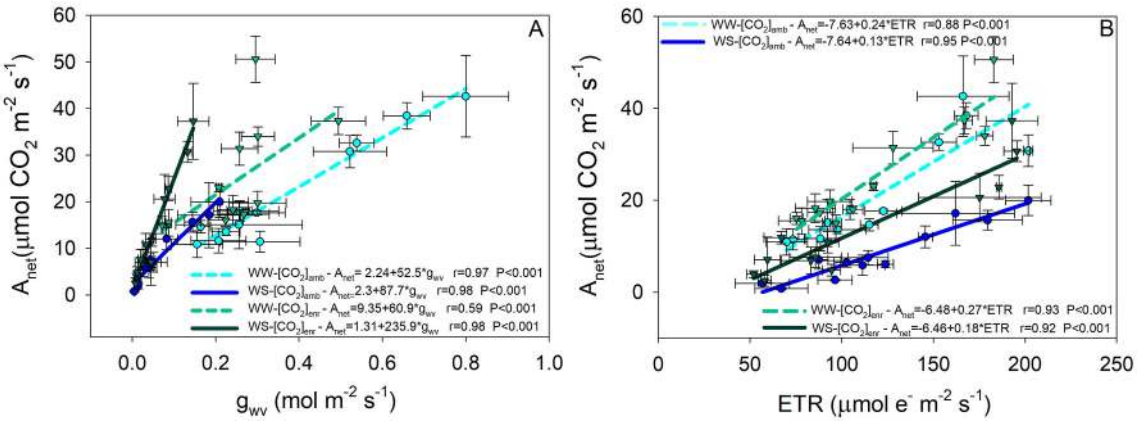

Fig. 2. Response of net photosynthesis to changes in stomatal conductance (A, A_{net} *vs.* g_{wv}) and electron transport rate (B, A_{net} *vs.* ETR) in *O. europaea* genotypes from three subspecies grouped according to two watering regimes and two [CO_2] growing concentrations. Symbols: Clear-blue: well-watered plants grown under ambient CO_2/WW – $[CO_2]_{amb}$; dark-blue: water-stressed plants grown under ambient CO_2/WS – $[CO_2]_{amb}$WW-$[CO_2]_{amb}$; Clear-green: well-watered plants grown under enriched CO_2/WW – $[CO_2]_{enr}$; Dark –green, water-stressed plants grown under enriched CO_2/WS – $[CO_2]_{enr}$. (For interpretation of the references to colour in this figure legend, the reader is referred to the Web version of this article.)

together. Leaf length (LL) and width (WL) (Supplementary Fig. S2), and the ratio LL/WL (data not shown) were influenced only by the genotype, without any impact of drought or CO_2 on the leaf morphology.

Among the genotypes, those from MAR showed the highest N_{mass} (Fig. 3B). Water stress promoted a significant increase in N for many of the genotypes. However, the most substantial effect came from the CO_2 (Supplementary Table S2), which reduced leaf N in most of the genotypes, except in those from MAR. The N_{mass} content ranged from 0.7 ± 0.1 % in ACZ8 (WS_$[CO_2]_{enr}$) to 2.4 ± 0.4 % in ACZ9 (WS_$[CO_2]_{amb}$) across the different watering x CO_2 treatments. The N_{area} displayed a similar trend to that of N_{mass} (Fig. 3C), without any significant impact from SLA as a modifier of leaf area nitrogen expression on an area basis (N_{area}). Leaf C_{mass} content showed a similarly broad range as N_{mass} across genotypes and treatments. It varied from 46 ± 0.8 % in ACZ8 (WW_$[CO_2]_{enr}$) to 60.5 ± 1.4 in MAR2 (WS_$[CO_2]_{enr}$) across the different watering x CO_2 treatments. It also increased in response to water stress for most genotypes, but only under $[CO_2]_{enr}$ (Supplementary Fig. S3), particularly in MAR genotypes.

The $\delta^{15}N$ varied much across genotypes, which was the main source of variation (Supplementary Table 2). Even though genotype was the most relevant source of variation (Fig. 4A), watering, CO_2 and their interactions, had also a significant effect on $\delta^{15}N$ denoting the complex effect of the interplay of all these factors on $\delta^{15}N$. In particular, the $\delta^{15}N$ exhibited high reactivity to water stress and CO_2 for most genotypes, ranging from −2 ± 0.1 ‰ in HER5 (WW _ $[CO_2]_{enr}$) to 3 ± 0.2 in MAR3 (WS _ $[CO_2]_{enr}$) across the different watering x CO_2 treatments. Despite the high variability observed for both leaf $\delta^{15}N$ and leaf N_{area} in response to all the studied factors (genotype, water availability and growth CO_2), a significant positive relationship between these two traits was found (Supplementary Fig. S4).

Water stress brought about a decrease in $\delta^{13}C$ for most of the genotypes. The $[CO_2]_{enr}$ promoted an increase in $\delta^{13}C$ over that under $[CO_2]_{amb}$ for many of the genotypes (Fig. 4B). The interplay between $\delta^{13}C$ and $\delta^{15}N$ across genotypes and treatments resulted in a negative relationship between both physiological traits (Fig. 4C). However, there were differences in the intercept according to watering and CO_2. The intercepts were higher for WS plants within each CO_2 treatment, and the difference between the intercepts between WW and WS was higher under $[CO_2]_{enr}$, showing a higher reactivity of $\delta^{13}C_{est}$ to a change in the $\delta^{15}N$ (Fig. 4C).

Differences in $\delta^{13}C$ should be interpreted cautiously, as the isotopic composition of the CO_2 of the atmosphere surrounding plants in each CO_2 growing environment was probably differentially depleted in C^{13}. To overcome this shortcoming, an approach of standardised axes for $\delta^{13}C$ was applied to establish the relationship between $\delta^{13}C$ with WUE_i and C_i/C_a across genotypes (Fig. 5A and B). This allowed comparing the relationship between variables upon standardising $\delta^{13}C$ values for each genotype according to the grand mean for each CO_2 environment. There was a positive relationship across genotypes between WUE_i and $\delta^{13}C$, but with a higher slope under $[CO_2]_{enr}$ (Fig. 5A). The Pattern was similar between C_i/C_a and $\delta^{13}C$, but in this case, the relationship was negative, although the slope under $[CO_2]_{enr}$ was also higher (Fig. 5B).

PNUE and WUE_i differed among genotypes. The WUE_i increased in most of the genotypes in response to water stress and to $[CO_2]_{enr}$ (Supplementary Fig. S5). However, PNUE followed the opposite pattern, decreasing with water stress, but increasing also in response to $[CO_2]_{enr}$. As result, we found a negative relationship between PNUE and WUE_i across genotypes. Although this relationship showed a higher intercept under $[CO_2]_{enr}$, which translated into higher PNUE for a specific WUE_i across watering regimes (Supplementary Fig. S4). This happened despite the trend to decrease leaf nitrogen content under $[CO_2]_{enr}$, except in those genotypes from MAR.

3.4. Total plant Water use

The water plant consumption standardised by the plant basal area (WC_s) was very sensitive to the VWC (Fig. 6). The CO_2 was relevant in decreasing WC_s across genotypes. The effect of VWC, genotype and CO_2 were highly significant on WC_s ($LR\chi^2_{(1)} = 1176.07$, $p < 0.001$; $LR\chi^2_{(11)} = 149.87$, $p < 0.001$; $LR\chi^2_{(1)} = 24.09$, $p < 0.001$, respectively). WC_s increased with VWC and decreased with CO_2 (Fig. 7).

The interactions VWC x genotype, VWC x CO_2, and genotype x CO_2 were also significant ($LR\chi^2_{(11)} = 50.88$, $p < 0.001$; $LR\chi^2_{(1)} = 16.53$, $p < 0.001$; $LR\chi^2_{(11)} = 28.01$, $p = 0.003$, respectively), denoting that the effect of VWC on WCs varied across genotypes and CO_2 levels. The third-order interaction VWC x genotype x CO_2 was not significant on WC_s ($LR\chi^2_{(11)} = 8.46$, $p = 0.67$). Although LAR was significantly different across the three factors: genotype, water availability and CO_2 (Supplementary Table S2 and Fig. S6), the effects of LAR, g_{wv} and g_{min} on specific consumption rates (WC_s) were not significant. The most parsimonious model was the one that included only main effects of the factors, excluding covariates (Supplementary Table S3).

Both water stress and elevated growth CO_2 significantly reduced specific water consumption rates ($P < 0.001$). Notably, we also observed significant inter-clonal variability in specific water consumption, even between genotypes of the same subspecies (Fig. 7). However, the absence of significant interaction effects (Supplementary Table S2)

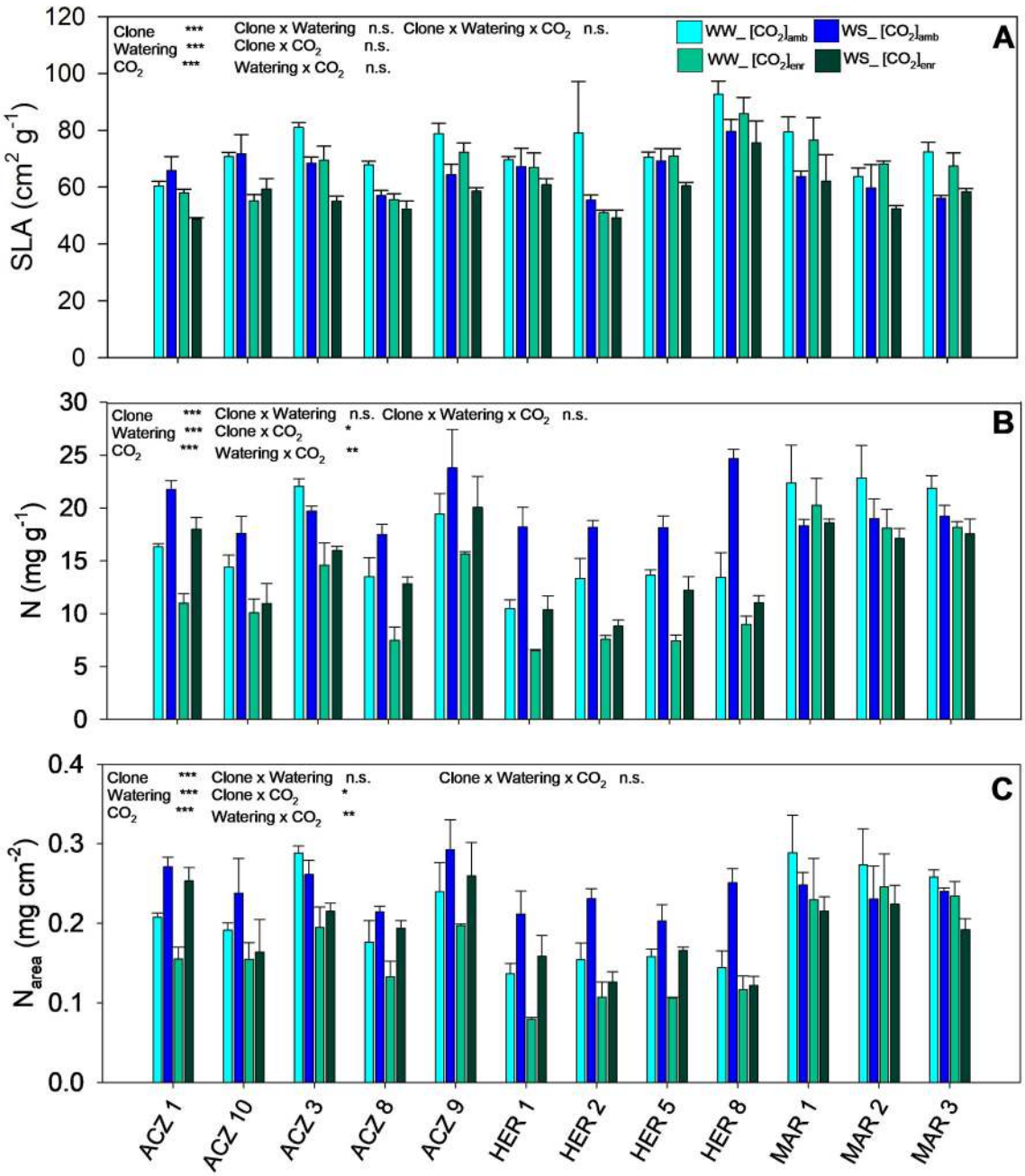

Fig. 3. (A) specific leaf area (SLA - $cm^2\ g^{-1}$); (B) Nitrogen content on a mass basis N_{mass} – %/g x $10^{-2}\ g^{-1}$), and (C) area basis (N_{area} - mg cm^{-2}) in leaves of 12 genotypes from 3 subspecies of *O. europaea* submitted to drought (D) or well-watered (WW), and growing under CO_2 ambient ($[CO_2]_{amb}$/400 ppm) or CO_2 enriched ($[CO_2]_{enr}$/800 ppm) atmospheres. Genotypes: ACZ1, ACZ10, ACZ3, ACZ8, ACZ9 subsp. e*uropaea*; HER1, HER2, HER5, HER8 subsp. *guanchica*; MAR1, MAR2, MAR3 subsp. *maroccana*. Clear-blue: WW – $[CO_2]_{amb}$; dark-blue: WW-$[CO_2]_{amb}$; Clear-green WW – $[CO_2]_{enr}$; Dark –green, D – $[CO_2]_{enr}$. Significance of the different factors from linear models was indicated as: $P < 0.001$ - ***, $P < 0.01$ - **, $P < 0.05$ – *, $P > 0.05$ non-significant – n.s. Bars indicate average values ± S.E. (n = 3). (For interpretation of the references to colour in this figure legend, the reader is referred to the Web version of this article.)

suggests that the impacts of water availability and CO_2 were similar across genotypes.

A more detailed analysis revealed the genotype-specific response to the progressive reduction in water consumption with the depletion of soil moisture availability in the pots (Fig. 7, and Supplementary Table S3). The genotype-specific response of WCs as a function of VWC took two different forms (i.e. linear and piecewise linear models). Other response functions (e.g. Michaelis-Menten, quadratic, hyperbola, etc) were tested but gave poorer fits (data not shown).

WCs of genotypes corresponding to subspecies ACZ and HER followed in general a piecewise linear response along the VWC range with a first steeper slope, a second more horizontal slope under higher VWC of pots and a breakpoint in between, while genotypes of subspecie MAR followed a linear response along the whole VWC range (Fig. 7). As a general pattern, first and second slopes were consistently lower under $[CO_2]_{enr}$ than under $[CO_2]_{amb}$, which means a lower water consumption for the same VWC in the former. Yet, the breakpoint was higher under $[CO_2]_{enr}$ than under $[CO_2]_{amb}$ (Supplementary Table S3). The genotypes of subspecies MAR and HER had higher first and second slopes than those of ACZ at both $[CO_2]_{amb}$ and $[CO_2]_{enr}$. Breakpoint differences between ACZ and HER were not found, and varied between 0.157 and 0.068 m^3m^{-3} among genotypes (Supplementary Table S3). Despite MAR

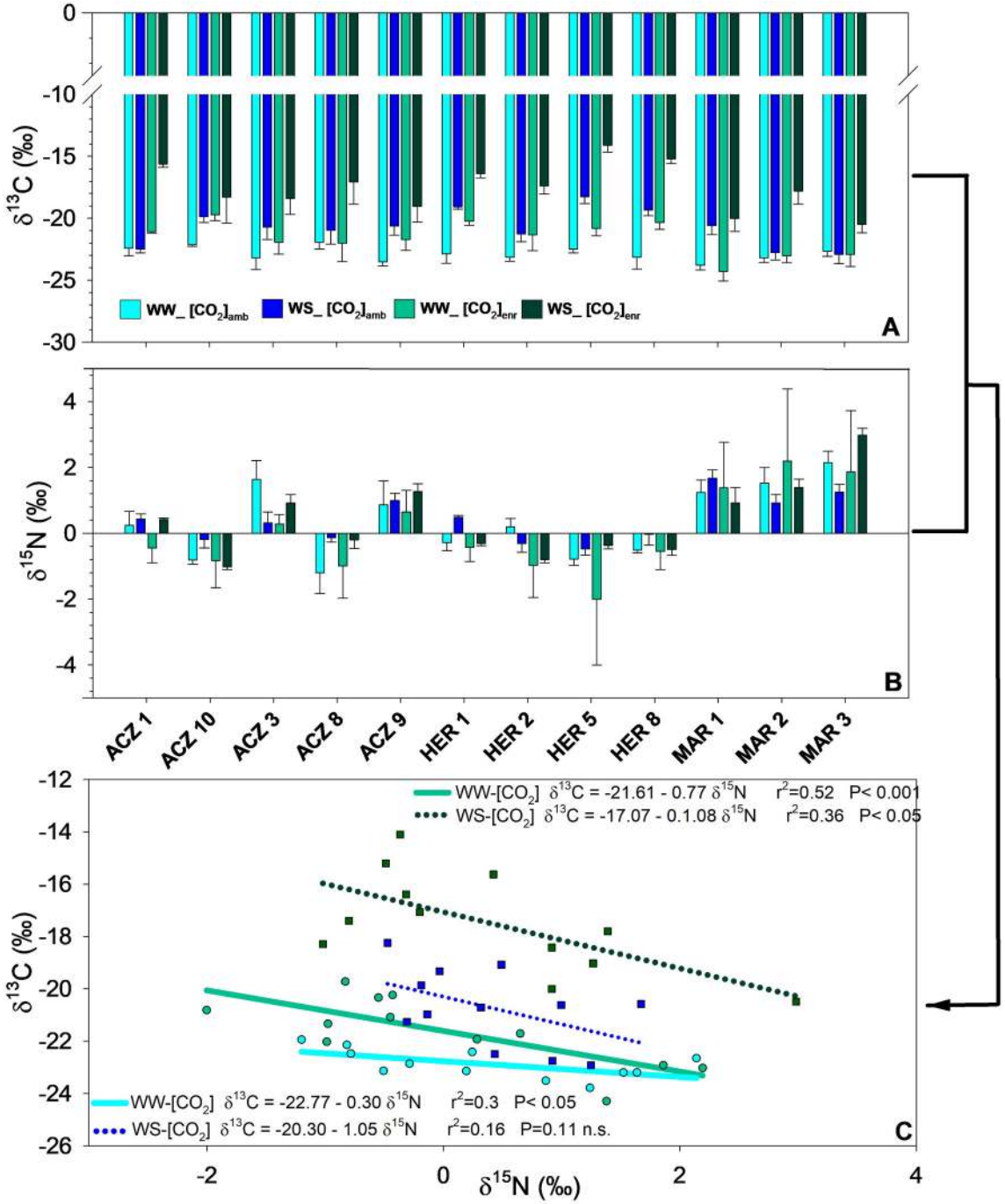

Fig. 4. (A) C^{13} isotopic composition ($\delta^{13}C$ - ‰); (B) N^{15} isotopic composition ($\delta^{15}N$ - ‰) in leaves of 12 genotypes from 3 subspecies of *O. europaea* submitted to drought (D) or well-watered (WW), and growing under CO_2 ambient ($[CO_2]_{amb}$/400 ppm) or CO_2 enriched ($[CO_2]_{enr}$/800 ppm) atmospheres. Genotypes: ACZ1, ACZ10, ACZ3, ACZ8, ACZ9 subsp. *europaea*; HER1, HER2, HER5, HER8 subsp. *guanchica*; MAR1, MAR2, MAR3 subsp. *maroccana*. Clear-blue: WW – $[CO_2]_{amb}$; dark-blue: WS-$[CO_2]_{amb}$; Clear-green WW – $[CO_2]_{enr}$; Dark – green D – $[CO_2]_{enr}$; (C) Relationships between $\delta^{13}C$ and $\delta^{15}N$ across genotypes and watering and CO_2 treatments. Significance of the different factors from lineal models was indicated as: $P < 0.001$ - ***, $P < 0.01$ - **, $P < 0.05$–0.05, non-significant – n.s. Linear regression models for the $\delta^{13}C$ and $\delta^{15}N$ relationships are depicted in Figure C; standard errors in Fig. 4C are omitted for clarity of the graph. Bars indicate average values ± S.E. (n = 3). (For interpretation of the references to colour in this figure legend, the reader is referred to the Web version of this article.)

genotypes having the highest WCs values at the upper part of the VWC range, they ranked lower than the rest of the genotypes at the middle and/or lower part of the VWC range. This resulted from the inter-clonal variation observed in the response functions of the relationship between WCs and VWC and differences in the slopes of those responses (Fig. 7).

3.5. Growth and biomass partitioning

Most growth-related traits changed according to genotype, watering and CO_2, except for CO_2, which was significant only for some growth traits (Supplementary Table S4). Height (He) of the different genotypes ranged between 122 ± 11.7 cm in ACZ10 under WW_ $[CO_2]_{enr}$ and 38.2 ± 1.2 cm in MAR1 under WW_ $[CO_2]_{amb}$. In general, genotypes from ACZ grew taller than those from MAR, and HER showed intermediate

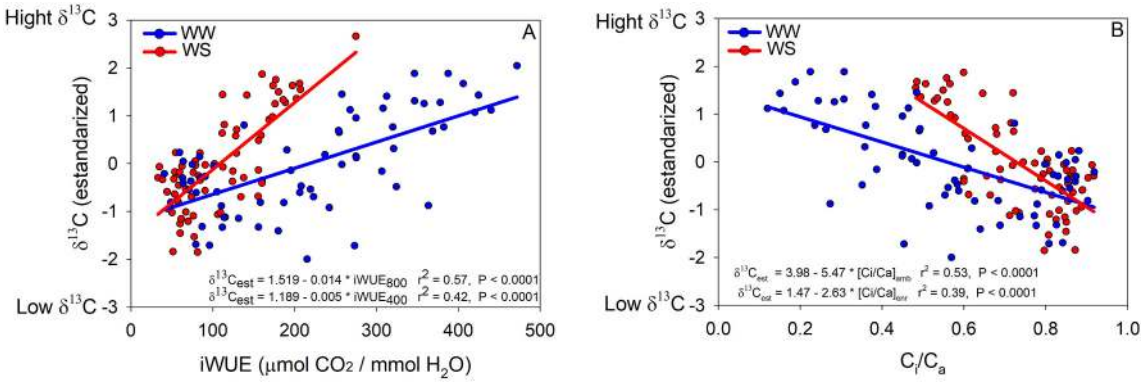

Fig. 5. Relationship between standardized leaf $\delta^{13}C$ values for plants of 12 wild olive genotypes growing under $[CO_2]_{amb}$ and $[CO_2]_{enr}$ atmospheres; (A) iWUE – intrinsic water use efficiency from leaf gas exchange, (B) Ci/Ca - ratio between intercellular and ambient CO_2. Blue points and lines represent plants grown under ambient 400 ppm $[CO_2]_{amb}$; Red points and lines represent plants grown under 800 ppm $[CO_2]_{enr}$. Data across genotypes and watering treatments were pooled to explore in more detail the impact of atmospheric CO_2 enrichment on the drivers affecting the standardised leaf $\delta^{13}C$. Note, leaf $\delta^{13}C$ was standardised to correct for the impoverishment in C^{13} of the air surrounding plants in the $[CO_2]_{enr}$ treatment during growth, which allowed for correction of the overall higher values of leaf $\delta^{13}C$ for plants growing at 800 ppm (see Fig. 4 for absolute values). (For interpretation of the references to colour in this figure legend, the reader is referred to the Web version of this article.)

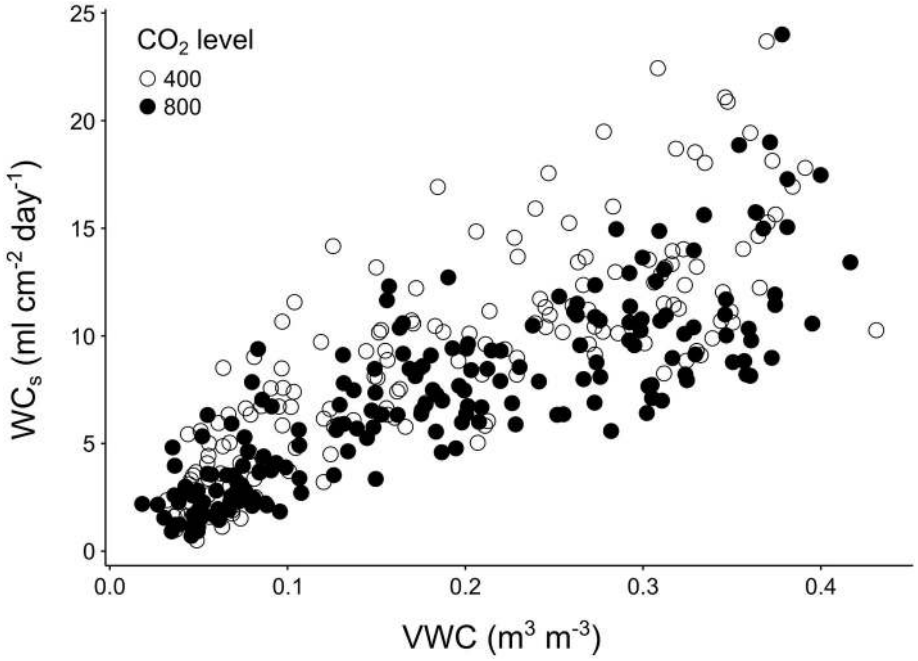

Fig. 6. Scatterplot of the water consumption standardised by the basal area of the plant at the collar root (WC_s - ml cm^{-2} day^{-1}) against the volumetric water content of the pots (VWC - m^3 m^{-3}) across twelve genotypes of *O. europaea* from three subspecies. Data considers the performance during the cycle of drought imposition. Growth under $[CO_2]_{enr}$ (black points) resulted in a lower daily consumption than in plants growing under $[CO_2]_{amb}$ (white points).

He. The three genotypes from MAR showed lower basal stem diameter (SD) and height at the end of the experiment. SD variation was mainly explained by clon and CO_2. It was highest for clon ACZ10 (17.4 ± 0.9 mm in WS_ $[CO_2]_{enr}$) and lowest for MAR1 (S6S5.2 ± 0.1 mm in WW_ $[CO_2]_{amb}$). $[CO_2]_{enr}$ tended to increase SD across genotypes as compared with $[CO_2]_{amb}$. However, water availability did not have a significant effect on SD. Branching of plants (Br), expressed as the number of branches attached to the main stem, differed significantly among genotypes and CO_2. Many two- and three-way interactions were also significant. In particular, some genotypes, such as ACZ9, showed a much lower branching than HER5, considering a similar height. This translates into a more compact aspect of the latter regardless of watering or CO_2. Total biomass (TB) changed a lot according to genotype (Fig. S7D), ranging from 204.5 ± 23 g in ACZ10 (WS _ $[CO_2]_{enr}$) to 8.2 ± 0.7 g in MAR1 (WW_ $[CO_2]_{amb}$). CO_2 of the growth atmosphere also impacted growth, with most of the genotypes accumulating more TB under $[CO_2]_{enr}$. Water stress negatively affected the TB, but not in all the genotypes. The three *maroccana* ssp genotypes (MAR1, MAR2, MAR3) showed not only the smallest size, but also the lowest TB, regardless of the watering or CO_2 (Supplementary Table 4, Fig. S7). The TB was positively correlated with the $\delta^{13}C$ across genotypes under WS and CO_2, though the relationship was stronger under WW (Supplementary Fig. S8).

Genotype was the main source of variation for the different biomass partitioning parameters (Supplementary Fig. S9). LWR also changed depending on the watering and CO_2, with a significant interaction between genotype and CO_2. In the case of SWR, watering was not significant, although the genotype and CO_2 were. The RWR was different

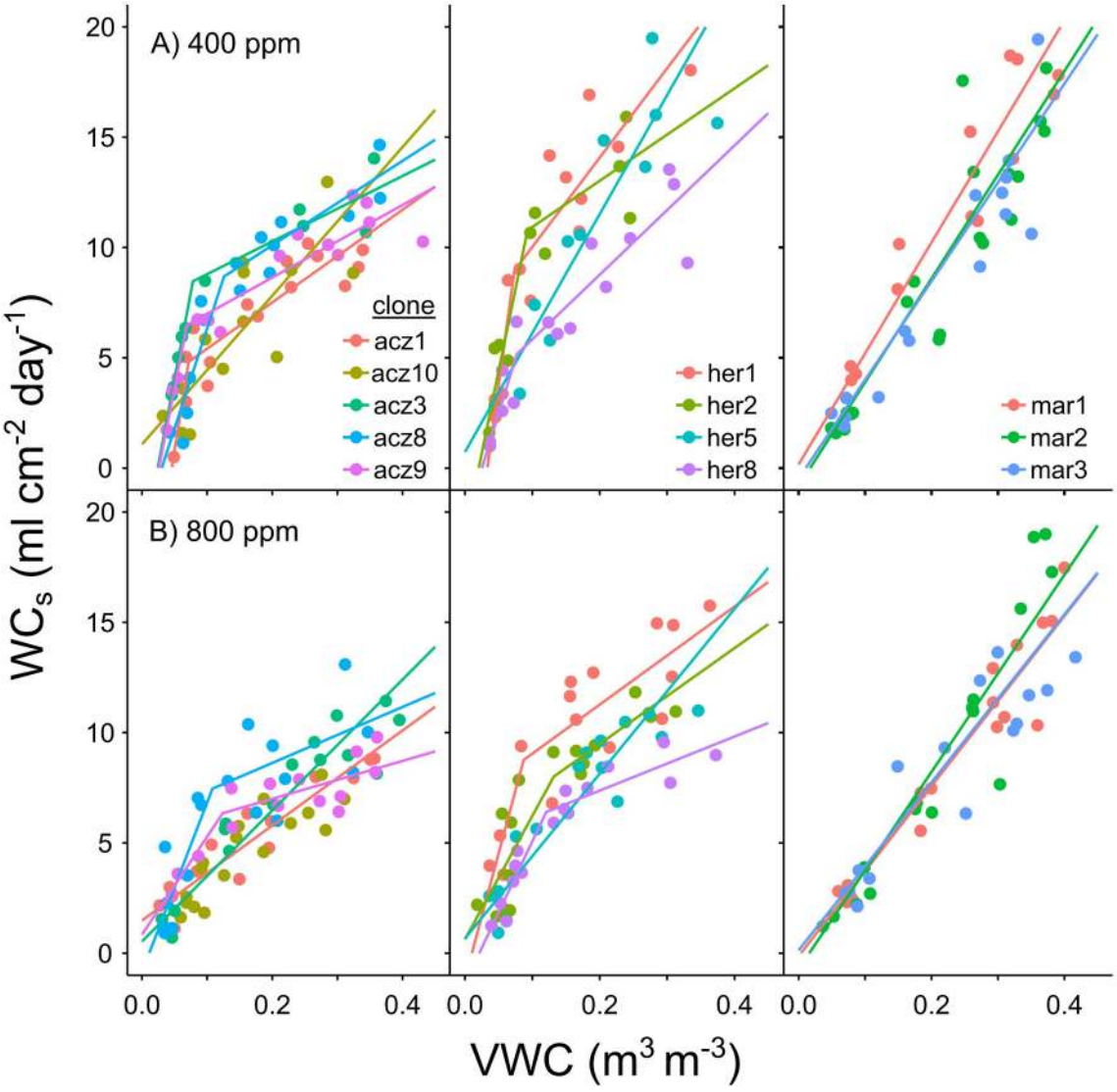

Fig. 7. Scatterplot of WCs against VWC split by subspecies of genotypes (ACZ1, ACZ10, ACZ3, ACZ8, ACZ9 subsp. europaea; HER1, HER2, HER5, HER8 subsp. guanchica; MAR1, MAR2, MAR3 subsp. maroccana) and CO_2 growing media; A) plants grown at 400 ppm, $[CO_2]_{amb}$; B) plants grown at 800 ppm, $[CO_2]_{enr}$. The lines denote the corresponding best-fit response functions for each genotype x CO_2 combination (see Table S4 for more details of models).

between genotypes, and watering explained more variation than for the LWR and SWR. The CO_2 was not significant for RWR, though the interactions genotype x watering, along with genotype x CO_2, were (Supplementary Table S2).

Huber value (H_v) changed in response to drought and genotype, with a lower influence of the CO_2. H_v was highest for individuals submitted to drought, and the three *maroccana* genotypes showed the highest H_v across treatments (Supplementary Table S4). CO_2 modified H_v only for well-watered plants in the two genotypes ACZ8, ACZ9.

3.6. Overall clonal differentiation and grouping in three subspecies

There were clear differences among genotypes when considering the pool of traits. Although the number of genotypes was low, differentiation based on subspecies was also observed in a PCA (Fig. 8). In fact, there was a distinct separation among subspecies in the first two components of the PCA under both CO2 atmospheres (Fig. 8).

The first component explained 40.68 % of the variance and showed a clear distinction between genotypes of the subspp. *europaea* and *maroccana*, with *guanchica* positioned intermediately and partly overlapping with *europaea*. The second and third components accounted for 15.90 % and 9.76 % of the variance, respectively, allowing differentiation between WW and WS plants and, to a lesser extent, between $[CO_2]_{amb}$ and $[CO_2]_{enr}$ growth environments. Variables such as TB, LA, LW, SD, Br, and LL had the highest positive loadings on the first principal component. Conversely, $\delta^{15}N$, ETR, A_{net}, H_v, RWR, and N exhibited the lowest negative loadings on the same component. These variables exerted the greatest influence on the positive and negative directions of the component, respectively.

4. Discussion

The wild olive is characterized by high genetic variability, comprising different subspecies from a complex evolutionary history (Besnard et al., 2013; Kassa et al., 2019; García-Verdugo et al., 2009; Díaz-Rueda et al., 2020). Unlike the numerous cultivated olive varieties, for which a substantial body of knowledge on their physiological response to various environmental stressors exists, information on the physiological performance of wild olive subspecies is considerably scarcer (Hernandez-Santana et al., 2019). Beyond general patterns across genotypes in modulating their drought response under atmospheric CO_2 enrichment, this study provides a comprehensive overview

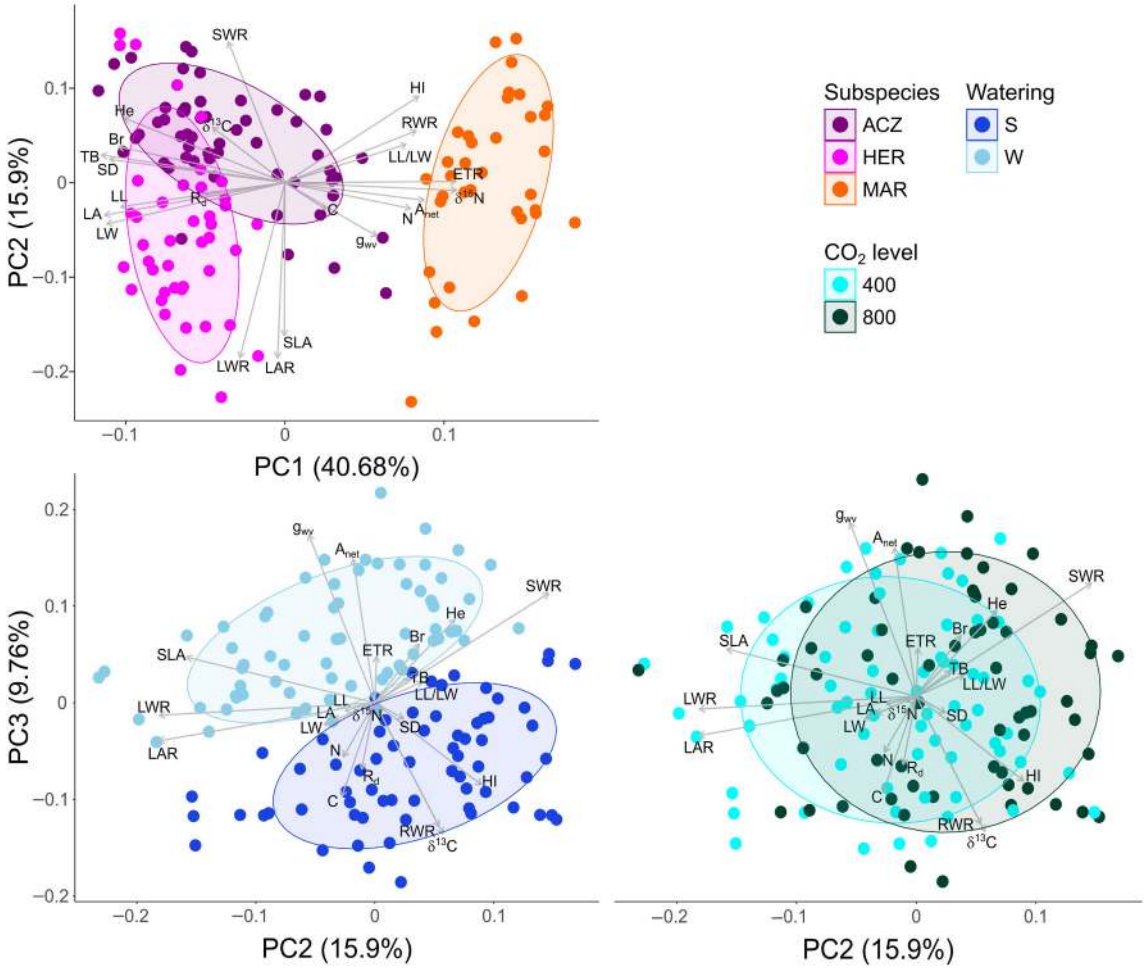

Fig. 8. Biplot of principal components showing factor coordinates of the studied traits. The variance explained by each principal components (PC) is indicated on the corresponding axis. Confidence ellipses are included to represent the variability within and separation between groups.

of the wide spectrum of strategies and physiological responses to drought exhibited by genotypes representative of three wild olive subspecies. Genotypes showed contrasting phenotypic variability and functional behaviours in response to water-stress conditions. The CO_2 enrichment of the atmosphere led to changes in the drought response at various levels of biological integration, from leaf-level interplay between carbon fixation and stomatal regulation of leaf water loss to overall plant behaviour (i.e. biomass accumulation and total plant water use). As expected, the evergreen wild olive demonstrated an enhancement in photosynthetic carbon uptake and growth for most genotypes under $[CO_2]_{enr}$ (Niinemets et al., 2011; De Souza et al., 2024). $[CO_2]_{enr}$ buffered the penalties on carbon fixing imposed by drought, alongside reductions in water loss at both leaf and plant levels. The findings of this study underscore the substantial variability observed in wild olive and its high phenotypic plasticity in response to drought. Nonetheless, certain general patterns were identified in the modulation of intrinsic water use efficiency and photosynthetic nitrogen use efficiency, both of which increased under $[CO_2]_{enr}$ across the pool of genotypes, as shown by leaf gas exchange measurements and leaf isotopic composition ($\delta^{13}C$, $\delta^{15}N$). The interaction between drought and $[CO_2]$ affected the plants' carbon and water economies, as well as nitrogen absorption and accumulation in the leaves. Our results are particularly relevant in light of the expected responsiveness of wild olive to two principal drivers of climate change in the Mediterranean region: drought and atmospheric CO_2 enrichment.

4.1. Sensitivity to water stress in wild olive genotypes, modulation from the leaf to the overall plant by the growing CO_2 of the atmosphere

Genotypes within subspecies represented the most significant source of phenotypic variation in response to water stress, underscoring the existence of different water usage strategies among individuals of the same species (De Miguel et al., 2012; Hernandez-Santana et al., 2019). Notably, high phenotypic plasticity in morpho-functional traits has previously been observed in wild olive genotypes in response to water stress. (Hernandez-Santana et al., 2019; García-Verdugo et al., 2023). Furthermore, some general patterns emerged across genotypes concerning the fine-tuning of water use efficiency from $\delta^{13}C$ and WUEi, both modulated by the interaction between drought and $[CO_2]$ enrichment of the atmosphere.

Responsiveness to CO_2 varied depending on genotype, but the dry-down cycle exerted a greater impact on leaf physiological and growth-related traits for most of them. Nonetheless, the CO_2 x watering interaction still revealed a significant interplay between both factors for many morpho-functional traits (Ainsworth and Rogers, 2007). Water stress reduced A_{net}, g_{wv} and ETR to a lesser extent, denoting that both photochemical and stomatal limitations affected A_{net} (Hernandez-Santana et al., 2019). Typically, g_{wv} decreased due to drought in most genotypes to a greater extent than A_{net} and ETR (Medeiros and Ward, 2013). Despite this, ETR remained as an important factor explaining variations in A_{net} across genotypes, regardless of water availability and CO_2 levels. The response varied among genotypes, and was influenced by atmospheric CO_2 enrichment (see below), with

different strategies in the stringency of stomatal control of leaf water loss and carbon uptake. Most genotypes showed a decrease in g_{wv} under elevated CO_2 under well-watered conditions (Ainsworth and Long, 2021), though some did not (Avila et al., 2020). The down-regulation of g_{wv} under increased atmospheric CO_2 is absent in some forest species (Avila et al., 2020; Duan et al., 2015), but common in others (Jiang et al., 2021; Johnson et al., 2002).

The genotypes generally adopted a water-saving strategy response to drought and atmospheric CO_2 enrichment, evident from leaf g_{wv} and overall plant water use, demonstrating coordination between leaf and whole-plant water use. Although A_{net}, and to a lesser extent, overall growth increased, water consumption at the plant level was reduced under $[CO_2]_{enr}$. Changes in the leaf area ratio and g_{wv} did not offset each other (i.e. not significant LAR in models explaining total water consumption), with g_{wv} having a larger influence on reducing total plant water consumption under a CO_2-enriched atmosphere. A more conservative water use across genotypes was evident at elevated CO_2, with lower water losses at leaf and plant levels across various soil moisture conditions (Paudel et al., 2018). Moreover, the relationships between total plant water use and soil volumetric water content (VWC) in most genotypes were steeper under $[CO_2]_{amb}$. Conversely, the relative increase in A_{net} with g_{wv} was greater under $[CO_2]_{enr}$ than under $[CO_2]_{amb}$ in well-watered plants, and even more so in water-stressed plants (i.e. the "low-Ci effect", c.f. Kelly et al., 2016). Likewise, $[CO_2]_{enr}$ enhanced the ETR (Avila et al., 2020; Goodfellow et al., 1997), fostering a higher carbon fixation across genotypes, likely due to an increase in the efficiency of PSI and PSII under CO_2-enriched atmospheres (commented by Gamage et al., 2018), along with suppression of photorespiration (i.e. reviewed recently in Foyer et al., 2025). This response was more pronounced under WS conditions, indicated by a higher intercept and slope in the A_{net}-ETR relationship, (see Fig. 2). Such better reactivity to drought involving the interplay between different leaf diffusional and photochemical leaf traits could enhance adaptability of the evergreen wild olive to $[CO_2]_{enr}$ in the future (Niinemets et al., 2011), and strengthens its capacity to buffer stressful conditions against increased intensity and recurrences of dry periods caused by climate change (Medeiros and Ward, 2013).

Plant growth improvement by CO_2 enrichment was moderate (22.4 % for the pool of genotypes in a range of 7.9 %–48.4, and considering data from WW plants), as it is often observed for WUE_i (Peñuelas et al., 2020; van der Sleen et al., 2015). Changes in WUE_i seem more related to improved C_i at the sites of carboxylation, especially driven by the increase of the CO_2 source in the atmosphere. Both $\delta^{13}C$ and WUE_i from punctual leaf gas exchange mainly reflected reductions in leaf and whole plant water losses, as noted elsewhere. However, enhancement of CO_2 also improved both $\delta^{13}C$ and WUE_i. In other studies, higher transpiring plant leaf area under $[CO_2]_{enr}$ balances the down-regulation of g_{wv}, resulting in a non-clear effect on soil moisture (Jiang et al., 2021). However, more conservative water use was observed at the whole plant level in a wide range of VWC_s under a $[CO_2]$ enriched atmosphere. Moreover, the involvement of higher ETR in carbon uptake, and an enhancement of the CO_2 source that improved carbon availability to the sites of fixation, compensated in part for the negative impact of drought on A_{net} until the point iWUE was highest for WS-$[CO_2]_{enr}$ plants. The improvement of WUEi from changes in C_i under CO_2-enriched atmospheres has been widely discussed (Kelly et al., 2016), and continues to be a subject of debate (Pastore et al., 2019; Voelker et al., 2016). Moderate drought effects appear buffered by CO_2 enrichment (Paudel et al., 2018), but under more severe water stress, this counterbalancing positive effect may blur (Duan et al., 2013). In our study, the slope relating A_{net} to g_{wv} across genotypes in WS was higher for plants grown under $[CO_2]_{enr}$ as aforementioned (Sage, 1994), indicating that drought's negative effects varied by genotype but were generally lower under CO_2 enrichment in the temporal window the experiment lasted. Under well-watered conditions, changes in A_{net} with g_{wv} across genotypes, and hence in the WUE_i, had a similar slope, which can be interpreted as an analogous sensitivity of g_{wv} to CO_2 under well-watered conditions (Medeiros and Ward, 2013). Despite this general pattern, we observed different strategies in regulating the leaf gas exchange under concurrent water stress and CO_2 enrichment. Most genotypes increased WUE_i with drought, but responses under $[CO_2]_{enr}$ were genotype-specific.

4.2. Interplay between nitrogen, water and carbon leaf economy

There was a clear interplay between leaf nitrogen and water economy (Plett et al., 2020). The leaf N_{mass} and N_{area} decreased in response to CO_2 enrichment of the atmosphere for most genotypes (Poorter et al., 2022), maybe as a consequence of reduction in leaf photorespiration under $[CO_2]$ enriched atmospheres in some cases (Wujeska-Klause et al., 2019). However, increased CO_2 availability compensated for this, leading to higher A_{net}. Moreover, the elemental leaf N content and N^{15} isotopic fractionation were positively related (Aranda et al., 2017; Yousfi et al., 2012). The $\delta^{15}N$ depends on different processes affecting nitrogen absorption, including microbiome activity, the N source in the soil, and various patterns of N^{15} discrimination during uptake and N assimilation (Craine et al., 2015; Kalcsits et al., 2014; Yousfi et al., 2012). Besides, the leaf $\delta^{15}N$ has been pointed out as a potential indicator of tolerance to drought as nitrogen absorption is limited under drought conditions (Aranda et al., 2017; Yousfi et al., 2012). However, our finding that genotype was the most relevant factor explaining leaf $\delta^{15}N$ highlights relevance of the intraspecific $\delta^{15}N$ variation in forest trees (Aranda et al., 2017; Hu et al., 2025), despite being less documented than in crops (Yousfi et al., 2012, 2013). In this respect, the three genotypes from MAR, together with ACZ3 and ACZ9 maintained a positive $\delta^{15}N$, coinciding with the highest leaf N_{mass} and N_{area}, and the general positive relationship between $\delta^{15}N$ and leaf nitrogen content across genotypes and treatments (Supplementary Fig. S4). However, we found that these clones, particularly those from MAR, did not exhibit the highest biomass accumulation or iWUE, despite their high A_{net} and leaf nitrogen content. Olive is known for its active secondary metabolism (Mechri et al., 2020), as are many other Mediterranean plants. We hypothesize that wild olive diverts a substantial fraction of carbon to secondary metabolism, although this point warrants direct testing in future studies.

Regardless of the mechanisms determining inter-clonal differences, it is important to note the relationship between $\delta^{13}C$ and $\delta^{15}N$ across different growing conditions, with the highest $\delta^{13}C$ values corresponding to the lowest $\delta^{15}N$ values (Spangenberg et al., 2020). This relationship reflects a complex link between carbon, water and nitrogen physiology (Aranda et al., 2017; Serret et al., 2018; Tcherkez, 2011). Besides, there was a trend to maintain higher $\delta^{13}C$ for a similar $\delta^{15}N$ under $[CO_2]_{enr}$ compared to $[CO_2]_{amb}$. For a similar WUE_i, this also translated into an increase in PNUE under $[CO_2]_{enr}$ relative to $[CO_2]_{amb}$. This was despite the large decrease in leaf nitrogen resulting from growing under $[CO_2]_{enr}$ (Supplementary Fig. S5).

4.3. Relevance of genotype-specific response and subspecies in determining the whole plant response to drought and CO_2

Changes in the physiology of genotypes were coordinated with morphological and growth-related traits. Thus, the rising atmospheric CO_2 during plant growth not only enhanced leaf carbon assimilation under WW and WS conditions, but led to a moderately higher plant dry biomass accumulation too (Ainsworth and Rogers, 2007; Duan et al., 2013; Walker et al., 2021). The CO_2 enrichment partially balanced the negative impact of drought on growth. Finally, the combined effects of CO_2 and drought affected both biomass and biomass partitioning among organs, with patterns varying among genotypes. Large genetic differences in biomass partitioning have been previously observed (Lahive et al., 2021; Maier et al., 2022). This was consistent with the variable architecture observed across genotypes and treatments, along with the

idiosyncratic performance of each genotype. This differential impact of CO_2 and drought on total and allocation biomass, depending on the genotype, is especially relevant from both ecological and agronomic perspectives (Ainsworth and Long, 2021; Norby, 2025).

The multivariate approach showed a grouping of genotypes according to subspecies origin, indicating three different strategies in water and carbon use, with a tendency towards more conservative responses under CO_2 enrichment depending on subspecies. The studied genotypes come from three distinct geographic origins, matching three well-described subspecies of *O. europaea*, and belong to the same monophyletic group widely distributed in North Africa and the Mediterranean Basin (Díaz-Rueda et al., 2020). The subspp. *europaea* and *guanchica* are diploid, while *maroccana* is a hexaploid and endemic to Morocco (Besnard et al., 2018; Medeiros and Ward, 2013; Rubio de Casas et al., 2006). Previous studies positioned *guanchica* as intermediate between *europaea* and *maroccana* for leaf morphological traits (leaf length, width and their ratio), which aligns with the patterns observed in our study. There was a high diversity in morphological, photochemical, growth-related and gas exchange features in the pool of genotypes studied. This was to be expected given the diversity previously observed in the SILVOLIFE collection (Díaz-Rueda et al., 2020; Hernandez-Santana et al., 2019), origin of the 12 genotypes for our study. The three genotypes from subspp. *maroccana* showed the highest photosynthetic capacity and leaf nitrogen content under both growth CO_2 environments, but otherwise the lowest iWUE (from gas exchange and $\delta^{13}C$). However, this highest carbon uptake capacity did not result in a higher biomass increment as reported for other evergreen species (De Souza et al., 2024), or even among conspecific individuals (Sánchez-Gómez et al., 2017). This might be linked to the aforementioned higher carbon diverting to different sinks from growth, allocation trade-offs (greater investment in root or woody tissues, reflected by higher RWR or Hv), fine-scale hydraulic constraints, or high maintenance and respiration costs. Regardless of the more differential response of MAR, it's important to remark that in adaptive terms nature provides different solutions for the same adaptive problem in the form of different plant trait assemblages. In this respect, the tested clones come from very different genetic backgrounds, and the assemblages of different traits respond to this pattern as the CO_2 x drought interaction resulted in different functional solutions.The trait combinations observed linking vigor, water-use efficiency, nitrogen economy and drought responsiveness, highlight the agronomic potential of wild olive genotypes. MAR genotypes, with relatively higher root biomass allocation, and selected ACZ/HER genotypes combining improved carbon gain and growth under $[CO_2]_{enr}$ and WS emerge as promising candidates for future rootstock and breeding programs, although their adaptive value in field conditions remains to be tested.

5. Conclusions

The study's findings underscore the substantial genetic variability and phenotypic plasticity observed in wild olive responding to drought and elevated CO_2 atmospheres. Both provide the basis for adaptation to future climatic scenarios. The study is particularly relevant in light of the wild olive's resilience to the anticipated pressures of climate change in a CO_2-enriched Mediterranean environment. It opens an opportunity to improve the genetic basis of olive in the face of climate change challenges.

In our experiment, CO_2 partially offset the negative influence of soil moisture availability on the carbon capacity uptake of the plant, and in the lowering of the leaf nitrogen content. Indeed, a more conservative performance regarding plant water use under $[CO_2]_{enr}$ was accompanied by the overall improved carbon uptake capacity (i.e. overall A_{net} increase without significant changes in R_d). Different physiological processes changed accordingly, for example, higher stringency in leaf stomatal control of water losses, total daily water use by the plant, and improved water use efficiency at both short and long term scales (i.e. WUEi and $\delta^{13}C$). However, beyond the general trend, we observed mostly genotype and, to a lesser extent, subspecies-specific patterns in many of the functional traits studied. This last point is particularly relevant, as large-scale models often rely on species-specific patterns or functional groups to predict vegetation responses in a CO_2-enriched world.

CRediT authorship contribution statement

I. Aranda: Writing – review & editing, Writing – original draft, Validation, Investigation, Funding acquisition, Formal analysis, Data curation, Conceptualization. **D. Sánchez-Gómez:** Writing – review & editing, Visualization, Validation, Investigation, Formal analysis, Data curation. **F.J. Cano:** Writing – review & editing, Investigation. **L. Quintanilla:** Writing – review & editing, Investigation, Funding acquisition, Conceptualization. **M. Del Rey-Granado:** Writing – review & editing, Investigation. **P. Díaz-Rueda:** Writing – review & editing, Resources. **J.M. Colmenero-Flores:** Writing – review & editing, Resources. **B. Fernandez de Simón:** Writing – review & editing, Investigation. **N. Fernandez del Saz:** Writing – review & editing, Investigation. **M. Ribas-Carbó:** Writing – review & editing, Resources, Methodology. **J. Gago:** Writing – review & editing, Project administration, Investigation, Funding acquisition, Conceptualization.

Declaration of competing interest

The authors declare that they have no known competing financial interests or personal relationships that could have appeared to influence the work reported in this paper.

Acknowledgements

We acknowledge support of the publication fee by the CSIC Open Access Publication Support Initiative through its Unit of Information Resources for Research (URICI). This research was funded by MCIN/AEI/10.13039/501100011033, national call 'Generación de Conocimiento' 2019–2020, project number PID2019-107434 GA-I00, and co-financed by TED2021-131947B-100 funded by the European Union (NextGeneration EU/PRTR). FJC acknowledges grant RYC2021-035064-I funded by MCIN/AEI/10.13039/501100011033 and "European Union NextGenerationEU/PRTR". We would like to thank two anonymous reviewers by their constructive comments that help to improve the final version of the work.

Appendix A. Supplementary data

Supplementary data to this article can be found online at https://doi.org/10.1016/j.plaphy.2025.110958.

Data availability

Data will be made available on request.

References

Adam, N.R., Wall, G.W., Kimball, B.A., Idso, S.B., Webber, A.N., 2004. Photosynthetic down-regulation over long-term CO_2 enrichment in leaves of sour orange (*Citrus aurantium*) trees. New Phytol. 163 (2), 341–347. https://doi.org/10.1111/j.1469-8137.2004.01104.x.

Ainsworth, E.A., Long, S.P., 2021. 30 years of free-air carbon dioxide enrichment (FACE): what have we learned about future crop productivity and its potential for adaptation? Glob. Change Biol. 27 (1), 27–49. https://doi.org/10.1111/gcb.15375.

Ainsworth, E.A., Rogers, A., 2007. The response of photosynthesis and stomatal conductance to rising [CO_2]: mechanisms and environmental interactions. Plant Cell Environ. 30 (3), 258–270. https://doi.org/10.1111/j.1365-3040.2007.01641.x.

Aranda, I., Bahamonde, H.A., Sánchez-Gómez, D., 2017. Intra-population variability in the drought response of a beech (*Fagus sylvatica* L.) population in the southwest of Europe. Tree Physiol. 37 (7), 938–949. https://doi.org/10.1093/treephys/tpx058.

Aranda, I., Cadahía, E., de Simón, B.F., 2020. Leaf ecophysiological and metabolic response in Quercus pyrenaica Willd seedlings to moderate drought under enriched CO2 atmosphere. J. Plant Physiol. 244, 153083. https://doi.org/10.1016/j.envexpbot.2025.106218.

Aranda, I., Martin-Benito, D., Sánchez-Gómez, D., De Simón, B.F., Gea-Izquierdo, G., 2024. Different drought-tolerance strategies of tree species to cope with increased water stress under climate change in a mixed forest. Physiol. Plantarum 176 (5), e14562. https://doi.org/10.1111/ppl.14562.

Araus, J.L., Febrero, A., Vendrell, P., 1991. Epidermal conductance in different parts of durum wheat grown under Mediterranean conditions: the role of epicuticular waxes and stomata. Plant Cell Environ. 14 (6), 545–558.

Avila, R.T., De Almeida, W.L., Costa, L.C., Machado, K.L.G., Barbosa, M.L., De Souza, R.P. B., Martino, P.B., Juárez, M.A.T., Marçal, D.M.S., Martins, S.C.V., Ramalho, J.D.C., DaMatta, F.M., 2020. Elevated air [CO2] improves photosynthetic performance and alters biomass accumulation and partitioning in drought-stressed coffee plants. Environ. Exp. Bot. 177, 104137. https://doi.org/10.1016/j.envexpbot.2020.104137.

Becklin, K.M., Walker, S.M., Way, D.A., Ward, J.K., 2017. CO_2 studies remain key to understanding a future world. New Phytol. 214 (1), 34–40. https://doi.org/10.1111/nph.14336.

Beerling, D.J., Heath, J., Woodward, F.I., Mansfield, T.A., 1996. Drought—CO_2 interactions in trees observations and mechanisms. New Phytol. 134 (2), 235–242. https://doi.org/10.1111/j.1469-8137.1996.tb04628.x.

Besnard, G., Khadari, B., Navascués, M., Fernández-Mazuecos, M., El Bakkali, A., Arrigo, N., Baali-Cherif, D., Brunini-Bronzini De Caraffa, V., Santoni, S., Vargas, P., Savolainen, V., 2013. The complex history of the olive tree: from late Quaternary diversification of Mediterranean lineages to primary domestication in the northern Levant. Proc. Biol. Sci. 280 (1756), 20122833. https://doi.org/10.1098/rspb.2012.2833.

Besnard, G., Terral, J.-F., Cornille, A., 2018. On the origins and do-mestication of the olive: A review and perspectives. Annals of Botany 121, 385–403. https://doi.org/10.1093/aob/mcx145.

Birami, B., Nägele, T., Gattmann, M., Preisler, Y., Gast, A., Arneth, A., Ruehr, N.K., 2020. Hot drought reduces the effects of elevated CO_2 on tree water-use efficiency and carbon metabolism. New Phytol. 226 (6), 1607–1621. https://doi.org/10.1111/nph.16471.

Coleman, J.S., McConnaughay, K.D.M., Bazzaz, F.A., 1993. Elevated CO2 and plant nitrogen-use: is reduced tissue nitrogen concentration size-dependent? Oecologia 93 (2), 195–200. https://doi.org/10.1007/BF00317671.

Craine, J.M., Brookshire, E.N.J., Cramer, M.D., Hasselquist, N.J., Koba, K., Marin-Spiotta, E., Wang, L., 2015. Ecological interpretations of nitrogen isotope ratios of terrestrial plants and soils. Plant Soil 396 (1–2), 1–26. https://doi.org/10.1007/s11104-015-2542-1.

Crous, K.Y., Wujeska-Klause, A., Jiang, M., Medlyn, B.E., Ellsworth, D.S., 2019. Nitrogen and phosphorus retranslocation of leaves and stemwood in a mature eucalyptus Forest exposed to 5 years of elevated CO2. Front. Plant Sci. 10, 664. https://doi.org/10.3389/fpls.2019.00664.

Cui, J., Zheng, M., Bian, Z., Pan, N., Tian, H., Zhang, X., Qiu, Z., Xu, J., Gu, B., 2024. Elevated CO2 levels promote both carbon and nitrogen cycling in global forests. Nat. Clim. Change 14 (5), 511–517. https://doi.org/10.1038/s41558-024-01973-9.

De Miguel, M., Sanchez-Gomez, D., Cervera, M.T., Aranda, I., 2012. Functional and genetic characterization of gas exchange and intrinsic water use efficiency in a full-sib family of Pinus pinaster Ait. In response to drought. Tree Physiol. 32 (1), 94–103. https://doi.org/10.1093/treephys/tpr122.

De Souza, V.F., Rasulov, B., Talts, E., Morfopoulos, C., Albuquerque, P.M., Junior, S.D., Niinemets, Ü., De Carvalho Gonçalves, J.F., 2024. Thermal sensitivity determines the effect of high CO2 on carbon uptake in Populus tremula and Inga edulis. Theoretical and Experimental Plant Physiology 36 (2), 199–213. https://doi.org/10.1007/s40626-024-00312-9.

Díaz-Rueda, P., Franco-Navarro, J.D., Messora, R., Espartero, J., Rivero-Núñez, C.M., Aleza, P., Capote, N., Cantos, M., García-Fernández, J.L., De Cires, A., Belaj, A., León, L., Besnard, G., Colmenero-Flores, J.M., 2020. SILVOLIVE, a germplasm collection of wild subspecies with high genetic variability as a source of rootstocks and resistance genes for olive breeding. Front. Plant Sci. 11, 629. https://doi.org/10.3389/fpls.2020.00629.

Díaz-Rueda, P., Cantos-Barragán, M., Colmenero-Flores, J.M., 2021. Growth quality and development of olive plants cultured in vitro under different illumination regimes. Plants 10 (10), 2214. https://www.mdpi.com/2223-7747/10/10/2214.

Duan, H., Amthor, J.S., Duursma, R.A., O'Grady, A.P., Choat, B., Tissue, D.T., 2013. Carbon dynamics of eucalypt seedlings exposed to progressive drought in elevated [CO2] and elevated temperature. Tree Physiol. 33 (8), 779–792. https://doi.org/10.1093/treephys/tpt061.

Duan, H., O'Grady, A.P., Duursma, R.A., Choat, B., Huang, G., Smith, R.A., Jiang, Y., Tissue, D.T., 2015. Drought responses of two gymnosperm species with contrasting stomatal regulation strategies under elevated [CO_2] and temperature. Tree Physiol. 35 (7), 756–770. https://doi.org/10.1093/treephys/tpv047.

Ellsworth, D.S., Reich, P.B., Naumburg, E.S., Koch, G.W., Kubiske, M.E., Smith, S.D., 2004. Photosynthesis, carboxylation and leaf nitrogen responses of 16 species to elevated pCO_2 across four free-air CO_2 enrichment experiments in forest, grassland and desert. Glob. Change Biol. 10 (12), 2121–2138. https://doi.org/10.1111/j.1365-2486.2004.00867.x.

Evans, J.R., 1989. Photosynthesis and nitrogen relationships in leaves of C3 plants. Oecologia 78 (1), 9–19. https://doi.org/10.1007/BF00377192.

Forner, A., Valladares, F., Bonal, D., Granier, A., Grossiord, C., Aranda, I., 2018. Extreme droughts affecting Mediterranean tree species' growth and water-use efficiency: the importance of timing. Tree Physiol. 38 (8), 1127–1137. https://doi.org/10.1093/treephys/tpy022.

Foyer, C., Wang, A., Shi, K., 2025. CO_2 signalling in plants. Phil. Trans. Biol. Sci. 380. https://doi.org/10.1098/rstb.2024.0247, 1927.

Gamage, D., Thompson, M., Sutherland, M., Hirotsu, N., Makino, A., Seneweera, S., 2018. New insights into the cellular mechanisms of plant growth at elevated atmospheric carbon dioxide concentrations. Plant Cell Environ. 41 (6), 1233–1246. https://doi.org/10.1111/pce.13206.

García-Verdugo, C., Douthe, C., Francisco, M., Ribas-Carbó, M., Flexas, J., Moreira, X., 2023. Does insular adaptation to subtropical conditions promote loss of plasticity over time? Perspect. Plant Ecol. Evol. Systemat. 58, 125713. https://doi.org/10.1016/j.ppees.2022.125713.

García-Verdugo, C., Fay, M.F., Granado-Yela, C., De Casas, R.R., Balaguer, L., Besnard, G., Vargas, P., 2009. Genetic diversity and differentiation processes in the ploidy series of *Olea europaea* L.: a multiscale approach from subspecies to insular populations. Mol. Ecol. 18 (3), 454–467. https://doi.org/10.1111/j.1365-294X.2008.04027.x.

Goodfellow, J., Eamus, D., Duff, G., 1997. Diurnal and seasonal changes in the impact of CO2 enrichment on assimilation, stomatal conductance and growth in a long-term study of Mangifera indica in the wet-dry tropics of Australia. Tree Physiol. 17 (5), 291–299. https://doi.org/10.1093/treephys/17.5.291.

Hartmann, H., Bastos, A., Das, A.J., Esquivel-Muelbert, A., Hammond, W.M., Martínez-Vilalta, J., McDowell, N.G., Powers, J.S., Pugh, T.A.M., Ruthrof, K.X., Allen, C.D., 2022. Climate change risks to global Forest health: emergence of unexpected events of elevated tree mortality worldwide. Annu. Rev. Plant Biol. 73 (1), 673–702. https://doi.org/10.1146/annurev-arplant-102820-012804.

Hernandez-Santana, V., Diaz-Rueda, P., Diaz-Espejo, A., Raya-Sereno, M.D., Gutiérrez-Gordillo, S., Montero, A., Perez-Martin, A., Colmenero-Flores, J.M., Rodriguez-Dominguez, C.M., 2019. Hydraulic traits emerge as relevant determinants of growth patterns in wild olive genotypes under water stress. Front. Plant Sci. 10, 291. https://doi.org/10.3389/fpls.2019.00291.

Hu, Y., Guy, R.D., Klápště, J., Lu, X., Soolanayakanahally, R.Y., 2025. Genetic and geographic determinants of nitrogen isotope discrimination in black cottonwood (*Populus trichocarpa*). Tree Physiol. https://doi.org/10.1093/treephys/tpaf072.

Jacobsen, A.L., Pratt, R.B., 2018. Extensive drought-associated plant mortality as an agent of type-conversion in chaparral shrublands. New Phytol. 219 (2), 498–504. https://doi.org/10.1111/nph.15186.

Jiang, M., Kelly, J.W.G., Atwell, B.J., Tissue, D.T., Medlyn, B.E., 2021. Drought by CO_2 interactions in trees: a test of the water savings mechanism. New Phytol. 230 (4), 1421–1434. https://doi.org/10.1111/nph.17233.

Johnson, J.D., Tognetti, R., Paris, P., 2002. Water relations and gas exchange in poplar and willow under water stress and elevated atmospheric CO_2. Physiol. Plantarum 115 (1), 93–100. https://doi.org/10.1034/j.1399-3054.2002.1150111.x.

Julca, I., Vargas, P., Gabaldón, T., 2023. Phylogenomics of the *Olea europaea* complex using 15 whole genomes supports recurrent genetic admixture together with differentiation into seven subspecies. BMC Biol. 21 (1), 85. https://doi.org/10.1186/s12915-023-01583-5.

Kalcsits, L.A., Buschhaus, H.A., Guy, R.D., 2014. Nitrogen isotope discrimination as an integrated measure of nitrogen fluxes, assimilation and allocation in plants. Physiol. Plantarum 151 (3), 293–304. https://doi.org/10.1111/ppl.12167.

Kassa, A., Konrad, H., Geburek, T., 2019. Molecular diversity and gene flow within and among different subspecies of the wild olive (Olea europaea L.): a review. Flora 250, 18–26. https://doi.org/10.1016/j.flora.2018.11.014.

Kelly, J.W.G., Duursma, R.A., Atwell, B.J., Tissue, D.T., Medlyn, B.E., 2016. Drought × CO_2 interactions in trees: a test of the low-intercellular CO_2 concentration (C_i) mechanism. New Phytol. 209 (4), 1600–1612. https://doi.org/10.1111/nph.13715.

Lahive, F., Handley, L.R., Hadley, P., Daymond, A.J., 2021. Climate change impacts on Cacao: genotypic variation in responses of mature Cacao to elevated CO2 and water deficit. Agronomy 11 (5), 818. https://doi.org/10.3390/agronomy11050818.

Lauriks, F., Salomón, R.L., De Roo, L., Goossens, W., Leroux, O., Steppe, K., 2022. Limited plasticity of anatomical and hydraulic traits in aspen trees under elevated CO2 and seasonal drought. Plant Physiology 188 (1), 268–284. https://doi.org/10.1093/plphys/kiab497.

Maier, C.A., Johnsen, K.H., Anderson, P.H., Palmroth, S., Kim, D., McCarthy, H.R., Oren, R., 2022. The response of coarse root biomass to long-term CO_2 enrichment and nitrogen application in a maturing *Pinus taeda* stand with a large broadleaved component. Glob. Change Biol. 28 (4), 1458–1476. https://doi.org/10.1111/gcb.15999.

Mas, E., Vilagrosa, A., Morcillo, L., Saurer, M., Valladares, F. y, Grossiord, C., 2024. Drought effects in Mediterranean forests are not alleviated by diversity-driven water source partitioning. J. Ecol. 112 (9), 2107–2122. https://doi.org/10.1111/1365-2745.14387.

Mechri, B., Tekaya, M., Hammami, M., Chehab, H., 2020. Effects of drought stress on phenolic accumulation in greenhouse-grown olive trees (Olea europaea). Biochem. Systematics Ecol. 92, 104112. https://doi.org/10.1016/j.bse.2020.104112.

Medeiros, J.S., Ward, J.K., 2013. Increasing atmospheric [CO_2] from glacial to future concentrations affects drought tolerance via impacts on leaves, xylem and their integrated function. New Phytol. 199 (3), 738–748. https://doi.org/10.1111/nph.12318.

Niinemets, Ü., Flexas, J., Peñuelas, J., 2011. Evergreens favored by higher responsiveness to increased CO2. Trends Ecol. Evol. 26 (3), 136–142. https://doi.org/10.1016/j.tree.2010.12.012.

Norby, R.J., 2025. Forest productivity response to elevated CO_2 in free-air CO_2 enrichment experiments: the 23 percent solution, revisited. New Phytol., 70162 https://doi.org/10.1111/nph.70162.

Norby, R.J., Loader, N.J., Mayoral, C., Ullah, S., Curioni, G., Smith, A.R., Reay, M.K., Van Wijngaarden, K., Amjad, M.S., Brettle, D., Crockatt, M.E., Denny, G., Grzesik, R.T., Hamilton, R.L., Hart, K.M., Hartley, I.P., Jones, A.G., Kourmouli, A., Larsen, J.R.,

et al., 2024. Enhanced woody biomass production in a mature temperate forest under elevated CO2. Nat. Clim. Change 14 (9), 983–988. https://doi.org/10.1038/s41558-024-02090-3.

Norman, JM, 1982. Simulation of microclimates. In: Hatfield, JL, Thomason, IJ) (Eds.), Biometeorology in Integrated Pest Management. Academic Press, New York, pp. 65–99.

Ofori-Amanfo, K.K., Klem, K., Veselá, B., Holub, P., Agyei, T., Juráň, S., Grace, J., Marek, M.V., Urban, O., 2023. The effect of elevated CO2 on photosynthesis is modulated by nitrogen supply and reduced water availability in *Picea abies*. Tree Physiol. 43 (6), 925–937. https://doi.org/10.1093/treephys/tpad024.

Pastore, M.A., Lee, T.D., Hobbie, S.E., Reich, P.B., 2019. Strong photosynthetic acclimation and enhanced water-use efficiency in grassland functional groups persist over 21 years of CO_2 enrichment, independent of nitrogen supply. Glob. Change Biol. 25 (9), 3031–3044. https://doi.org/10.1111/gcb.14714.

Paudel, I., Halpern, M., Wagner, Y., Raveh, E., Yermiyahu, U., Hoch, G., Klein, T., 2018. Elevated CO2 compensates for drought effects in lemon saplings via stomatal downregulation, increased soil moisture, and increased wood carbon storage. Environ. Exp. Bot. 148, 117–127. https://doi.org/10.1016/j.envexpbot.2018.01.004.

Peñuelas, J., Fernández-Martínez, M., Vallicrosa, H., Maspons, J., Zuccarini, P., Carnicer, J., Sanders, T.G.M., Krüger, I., Obersteiner, M., Janssens, I.A., Ciais, P., Sardans, J., 2020. Increasing atmospheric CO2 concentrations correlate with declining nutritional status of European forests. Commun. Biol. 3 (1), 125. https://doi.org/10.1038/s42003-020-0839-y.

Plett, D.C., Ranathunge, K., Melino, V.J., Kuya, N., Uga, Y., Kronzucker, H.J., 2020. The intersection of nitrogen nutrition and water use in plants: new paths toward improved crop productivity. J. Exp. Bot. 71 (15), 4452–4468. https://doi.org/10.1093/jxb/eraa049.

Poorter, H., Knopf, O., Wright, I.J., Temme, A.A., Hogewoning, S.W., Graf, A., Cernusak, L.A., Pons, T.L., 2022. A meta-analysis of responses of C_3 plants to atmospheric CO_2: Dose–response curves for 85 traits ranging from the molecular to the whole-plant level. New Phytol. 233 (4), 1560–1596. https://doi.org/10.1111/nph.17802.

Ramsey, J., 2011. Polyploidy and ecological adaptation in wild yarrow. Proceedings of the National Academy of Sciences USA 108 (17), 7096–7101. https://doi.org/10.1073/pnas.1016631108.

Sánchez-Gómez, D., Mancha, J.A., Cervera, M.T., Aranda, I., 2017. Inter-genotypic differences in drought tolerance of maritime pine are modified by elevated [CO2]. Ann. Bot. 120 (4), 591–602. https://doi.org/10.1093/aob/mcx080.

Sattler, M.C., Carvalho, C.R., Clarindo, W.R., 2016. The polyploidy and its key role in plant breeding. Planta 243 (2), 281–296. https://doi.org/10.1007/s00425-015-2450-x.

Serret, M.D., Yousfi, S., Vicente, R., Piñero, M.C., Otálora-Alcón, G., Del Amor, F.M., Araus, J.L., 2018. Interactive effects of CO2 concentration and water regime on stable isotope signatures, nitrogen assimilation and growth in sweet pepper. Front. Plant Sci. 8, 2180. https://doi.org/10.3389/fpls.2017.02180.

Spangenberg, J.E., Schweizer, M., Zufferey, V., 2020. Shifts in carbon and nitrogen stable isotope composition and epicuticular lipids in leaves reflect early water-stress in vineyards. Sci. Total Environ. 739, 140343. https://doi.org/10.1016/j.scitotenv.2020.140343.

Tcherkez, G., 2011. Natural 15N/14N isotope composition in C3 leaves: are enzymatic isotope effects informative for predicting the 15N-abundance in key metabolites? Funct. Plant Biol. 38 (1), 1. https://doi.org/10.1071/FP10091.

Tegeder, M., Masclaux-Daubresse, C., 2018. Source and sink mechanisms of nitrogen transport and use. New Phytol. 217 (1), 35–53. https://doi.org/10.1111/nph.14876.

Tognetti, R., Sebastiani, L., Vitagliano, C., Raschi, A., Minnocci, A., 2001. Responses of two olive tree (Olea Europaea L.) cultivars to elevated CO_2 concentration in the field. Photosynthetica 39 (3), 403–410. https://doi.org/10.1023/A:1015186411662.

Voelker, S.L., Brooks, J.R., Meinzer, F.C., Anderson, R., Bader, M.K.-F., Battipaglia, G., Becklin, K.M., Beerling, D., Bert, D., Betancourt, J.L., Dawson, T.E., Domec, J., Guyette, R.P., Körner, C., Leavitt, S.W., Linder, S., Marshall, J.D., Mildner, M., Ogée, J., et al., 2016. A dynamic leaf gas-exchange strategy is conserved in woody plants under changing ambient CO_2: evidence from carbon isotope discrimination in paleo and CO_2 enrichment studies. Glob. Change Biol. 22 (2), 889–902. https://doi.org/10.1111/gcb.13102.

Walker, A.P., De Kauwe, M.G., Bastos, A., Belmecheri, S., Georgiou, K., Keeling, R.F., McMahon, S.M., Medlyn, B.E., Moore, D.J.P., Norby, R.J., Zaehle, S., Anderson-Teixeira, K.J., Battipaglia, G., Brienen, R.J.W., Cabugao, K.G., Cailleret, M., Campbell, E., Canadell, J.G., Ciais, P., et al., 2021. Integrating the evidence for a terrestrial carbon sink caused by increasing atmospheric CO_2. New Phytol. 229 (5), 2413–2445. https://doi.org/10.1111/nph.16866.

Wang, L., 2024. Global plant nitrogen use is controlled by temperature. Nat. Commun. 15 (1), 7651. https://doi.org/10.1038/s41467-024-50803-1.

Wang, L., Zheng, J., Wang, G., Dang, Q.-L., 2022. Increased leaf area compensated photosynthetic downregulation in response to elevated CO_2 and warming in white birch. Can. J. For. Res. 52 (8), 1176–1185. https://doi.org/10.1139/cjfr-2022-0076.

Warren, C.R., Aranda, I., Cano, F.J., 2011. Responses to water stress of gas exchange and metabolites in *Eucalyptus* and *Acacia* spp. Plant Cell Environ. 34 (10), 1609–1629. https://doi.org/10.1111/j.1365-3040.2011.02357.x.

Wujeska-Klause, A., Crous, K.Y., Ghannoum, O., Ellsworth, D.S., 2019. Lower photorespiration in elevated CO_2 reduces leaf N concentrations in mature *Eucalyptus* trees in the field. Glob. Change Biol. 25 (4), 1282–1295. https://doi.org/10.1111/gcb.14555.

Wullschleger, S.D., Tschaplinski, T.J., Norby, R.J., 2002. Plant water relations at elevated CO_2 – implications for water-limited environments. Plant Cell Environ. 25 (2), 319–331. https://doi.org/10.1046/j.1365-3040.2002.00796.x.

Yousfi, S., Serret, M.D., Araus, J.L., 2013. Comparative response of δ^{13} C , δ^{18} O and δ^{15} N in durum wheat exposed to salinity at the vegetative and reproductive stages. Plant Cell Environ. 36 (6), 1214–1227. https://doi.org/10.1111/pce.12055.

Yousfi, S., Serret, M.D., Márquez, A.J., Voltas, J., Araus, J.L., 2012. Combined use of δ^{13} C, δ^{18} O and δ^{15} N tracks nitrogen metabolism and genotypic adaptation of durum wheat to salinity and water deficit. New Phytol. 194 (1), 230–244. https://doi.org/10.1111/j.1469-8137.2011.04036.x.